WARMING UP

Innovatief Duurzaam Warmtecollectief

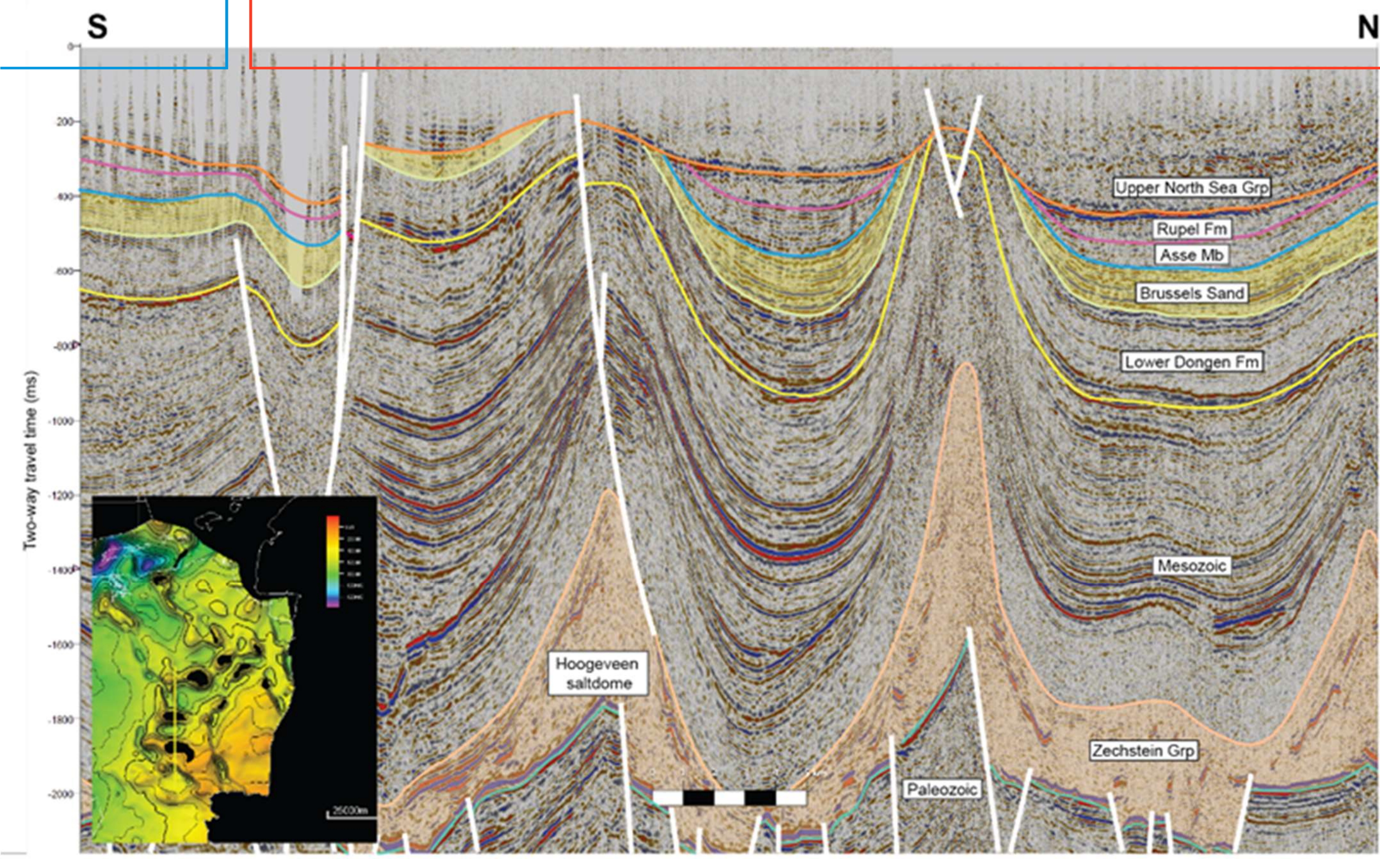

Mapping of the Brussels Sand Member in the Netherlands

door

Harald de Haan, Johan ten Veen, Sander Houben, Andreas Kruisselbrink

21 december 2020

Mapping of the Brussels Sand Member in the Netherlands

Harald de Haan, Johan ten Veen, Sander Houben, Andreas Kruisselbrink

21 december 2020

Kwaliteitsborger(s)
Hans Veldkamp

Dit project is uitgevoerd als onderdeel van het Innovatieplan WarmingUP. Dit is mede mogelijk gemaakt door subsidie van de Rijksdienst voor Ondernemend Nederland (RVO) in het kader van de subsidieregeling Meerjarige Missiegedreven Innovatie Programma's (MMIP), bij RVO bekend onder projectnummer TEUE819001.
WarmingUP geeft invulling aan MMIP-4 – Duurzame warmte en koude in gebouwde omgeving en levert daarmee een bijdrage aan Missie B – Een CO_2-vrije gebouwde omgeving in 2050.

Projectnummer
060.43190/01.01.01

Keywords
Brussels Sand, Distribution, Aquifer, Mapping, Geothermal, Low Enthalpy Geothermal

Jaar van publicatie
2020

Meer informatie
Lies Peters
T +31611012687
E lies.peters@tno.nl

December 2020 ©

Alle rechten voorbehouden. Niets uit deze uitgave mag worden verveelvoudigd, opgeslagen in een geautomatiseerd gegevens bestand, of openbaar gemaakt, in enige vorm of op enige wijze, hetzij elektronisch, mechanisch, door fotokopieën, opnamen, of enig andere manier, zonder voorafgaande schriftelijke toestemming van de uitgever.

Table of contents

1 Samenvatting (NL)

Het Zand van Brussel Laagpakket (ZBL) is een potentieel doel voor geothermische productie in Nederland. Om het potentieel van deze geothermische play te voorspellen zijn aanwezigheid, diepte en dikte van dit stratigrafische interval belangrijke parameters. Dit rapport beschrijft de resultaten van een karteringsproject waarin gebruik is gemaakt van zowel put als seismische data om de kaarten van het ZBL, zoals die momenteel in de ThermoGIS applicatie worden gebruikt, te actualiseren. Vorige projecten gebruikten alleen put data als input.

De consistentie van de huidige top en basis ZBL in putten is gecontroleerd. De top en basis van dit interval zijn op seismische data geïnterpreteerd en gecorreleerd. Logcorrelatie in putten laat zien dat het ZBL in Nederland uit drie sequenties bestaat waarvan in het verleden alleen de top van de bovenste eenheid op een consistente manier is geïnterpreteerd. De basis van het ZBL was op een inconsistente manier geïnterpreteerd doordat lokaal de basis van het ZBL was gedefinieerd aan de basis van de onderste sequentie en in andere regio's aan de basis van de middelste sequentie. In deze studie is de basis van het ZBL op een consistente wijze geïnterpreteerd, tenminste voor de putten die logs hebben van voldoende kwaliteit. In het zuidelijke studiegebied is de basis van de onderste sequentie als basis van het ZBL genomen en in het noordelijke gebied de basis van de middelste sequentie, omdat de basis van de onderste sequentie niet goed te volgen is op seismiek in dit gebied. De netto dikte van de onderste sequentie is berekend om het mogelijk te maken om de dikte van het ZBL in beide studiegebieden met elkaar te kunnen vergelijken.

De ruime beschikbaarheid van 3D en 2D seismische data maakt het mogelijk om het ZBL over heel Nederland te karteren. De verbreiding van het ZBL is beperkt tot het noordelijk, oostelijk en zuidwestelijk deel van Nederland. Het ZBL is afwezig in een WNW - OZO strekkende strook van 60 tot 100 km breed, lopende van Noord Holland tot Limburg. In dit gebied is het ZBL geërodeerd voordat jongere eenheden zijn afgezet. Het gebruik van seismische data maakt het mogelijk om de begrenzing waar het ZBL aanwezig is nauwkeuriger vast te stellen dan wanneer alleen putten worden gebruikt. Een vergelijking tussen de dikte van het ZBL in de seismiek en in de putten verbeterde de interpretatie van de basis van het ZBL in sommige putten.

De tijd-interpretatie van de seismische data is geconverteerd naar diepte. Hierbij is gebruik gemaakt van de parameters van het nationale snelheidsmodel VELMOD 3.1 nadat de validiteit en toepasbaarheid voor het ZBL zijn vastgesteld. De dieptevlakken van top en basis ZBL zijn aan de putten gekalibreerd om een goede overeenstemming te bereiken.

De belangrijkste verbeteringen zijn gerealiseerd in de dieptekaart van de basis van het ZBL met als gevolg een verbetering van de diktekaart. Het verloop van de dikte laat aanzienlijk minder abrupte diktevariaties zien dan in de voorgaande kaarten, die als gevolg van inconsistenties in put interpretaties "bull's-eyes " lieten zien. Ook de begrenzing van het ZBL langs de WNW - OZO strekkende strook van 60 tot 100 km breed is sterk verbeterd.

2 Summary

The Brussels Sand Member (BSM) is a potential target for geothermal projects in the Netherlands. To predict the potential of this geothermal play the presence, depth and thickness of this stratigraphic interval are important parameters. This report describes the results of a mapping project that used both well- and seismic data to update the maps of the BSM that are currently used in the ThermoGIS application. Previous maps only had well data as input.

The consistency of the current top and base of the BSM in wells was checked and the top and base of this interval were interpreted (“picked”) and correlated on seismic data. Well log correlation shows that the BSM in the Netherlands consists of three sequences of which only the top of the upper one was picked in a consistent way in the past. The base of the BSM was inconsistently picked: locally the base of the lowermost sequence was picked and in other regions the base of the middle cycle. For this study, the BSM is now consistently interpreted, at least for wells with well logs of sufficient quality. For the southern study area, the base of the lowermost sequence was taken as the base of the BSM. For the northern study area, the base of the middle sequence was taken as the base of the BSM, because the base of the lowermost sequence is not sufficiently visible on seismic data.in this area. A net thickness for the lowermost sequence has been calculated in order to be able to compare thicknesses in the two study areas.

The wide availability of (3D and 2D) seismic data made it possible to map the BSM across the entire Netherlands. The distribution of the BSM is limited to the northern, eastern and southwestern parts of the Netherlands. There is a 60-100 km wide WNW-ESE trending strip running from North Holland to Limburg where the BSM is absent. In this area the BSM was eroded before younger units were deposited. The use of seismic data made it possible to better pinpoint the boundary of the area in which the BSM is present. A comparison of the seismic and well thickness improved the picking of the base of the BSM in some wells.

The time interpretation of the seismic data was converted to depth by using parameters from the national velocity model VELMOD 3.1 after checking its validity and applicability for the BSM. The depth surfaces of top and base BSM were tied to the wells to ensure a good fit.

Improvements are mainly seen in the thickness map and the depth map of the base of the BSM, showing a smoother thickness distribution than in previous maps which suffered from inconsistencies in well picks that lead to bull’s-eyes in the thickness map. Another important improvement is a better definition of the boundary polygon enclosing the distribution of the BSM.

3 Introduction

In the Climate Agreement, it has been agreed that 1.5M houses need to be heated sustainably in 2030. Heating of these houses is currently done using natural gas. Part of these houses will be heated using collective heat networks and geothermal energy is an important source of heat for such networks. Within the WarmingUp project Theme 4, the goal is to accelerate the development and use of geothermal sources for use in urban heat networks. The following 3 main aspects are addressed:

1. Reduction of the geological risk through improved characterisation of the relatively poorly studied shallow subsurface and of marginal reservoirs, fit-for-purpose well designs and integration in heat networks
2. Quantification and control of the risk of induced seismicity and other effects on the environment.
3. Improved performance through optimisation of the production process.

The improved characterisation will primarily be made available via ThermoGIS (thermogis.nl). The goal of ThermoGIS is to present a regional geothermal resource assessment (Vrijlandt et al., 2019) to facilitate the use of geothermal resources. The study reported here focuses on improving the characterisation of the shallow subsurface: approximately 500 – 1500 m deep. In the Netherlands, within this depth range, mainly deposits of Cenozoic age are found (North Sea Groups). Of these formations, The Brussels Sand Member is expected to be the most prolific reservoir and therefore a prime focus in the project. Improving the characterisation of this reservoirs starts with accurate mapping of the depth and thickness, which is reported here.

The results of mapping the Dutch subsurface geology are traditionally represented in the national Digital Geological Model (DGM-Deep). To date, for the Cenozoic interval only the base of the Paleogene (Lower and Middle North Sea Groups) and the Neogene (Upper North Sea Group) are systematically mapped. The ThermoGIS application, however, needs more detailed information on distribution and thickness of aquifers. Traditionally, the bases and thicknesses of these aquifers were interpolated between wells to provide depth and thickness maps which naturally lack spatial detail in between the wells. The only way to update and improve the maps of the Brussels Sand Member is therefore by making use of seismic data, and to check the consistency of the lithostratigraphic well marker interpretations of the top and base of the Brussels Sand Member. In this report the **Brussels Sand Member** will be indicated by the abbreviation **BSM**.

In this mapping subproject of the WarmingUP project focus has been on three topics:

1. well stratigraphic interpretations were reviewed and updated;
2. a selection of seismic data has been interpreted;
3. top, base and thickness maps were modelled from the interpreted well and seismic data.

The general workflow applied here is common practice in oil and gas exploration and includes the interpretation of horizons from 3D and 2D seismic data in the time domain (two way travel time) (Figure 3-1). Subsequently, a conversion to the depth domain is made using a velocity model built from well log and checkshot data. The (re)interpreted well markers help to identify the horizons in the seismic data and they provide an anchor point for a tie to the correct depth at the well location after time-depth conversion. The depth converted and well-tied results have been integrated in a set of maps of the top, base and thickness of the BSM.

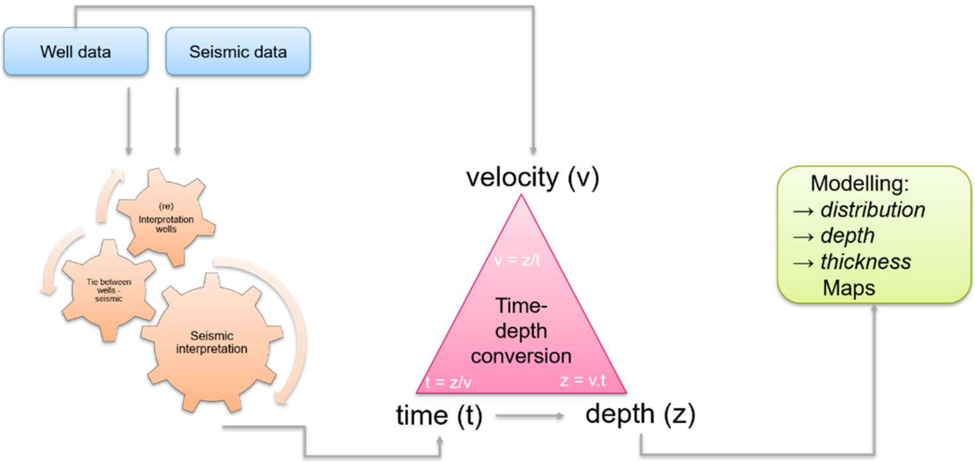

Figure 3-1 Schematic impression of the process to map the BSM. The linking process between the seismic data in time and the well data and depth maps is the time-depth conversion process that makes use of a velocity model.

4 Stratigraphic interpretations and update of well markers

4.1 Paleogeographic setting and climate

During the Early Paleogene (Paleocene-Eocene), the present-day area of the Netherlands was covered by a shallow sea. A deeper marine basin developed to the North, in the area of present-day Denmark and the northern Dutch offshore. This is related to the progressive opening of the Atlantic Ocean over the course of the Early Paleogene. Eustatic sea-level variations together with regional subsidence and uplift trends led to the development of a mosaic of shallow to open marine strata in the area of present-day onshore the Netherlands. During most of the Early Eocene, marine silt- and mudstones were deposited (the Ieper Clay in Netherlands and Belgium and the London Clay in the UK, Gibbard and Lewin, 2016). These are the result of intense chemical weathering under warm and humid climatic conditions (Collinson and Cleal, 2001a-b; Sluijs et al., 2008). This clay-dominated deposition was interrupted by a relatively abrupt northward expansion of shallow marine and deltaic sand complexes towards the north in the late Ypresian-Lutetian (early Middle Eocene). In the Netherlands, lower Middle Eocene (Lutetian) marine sandstone deposits are known as the Brussels Sand Member (BSM) whereas in Belgium the Brussels Sand is also developed as deltaic and fluvial facies types.
In terms of paleogeography, these sandstones were thought to predominantly originate from a southerly source, an assumption supported by the development of more proximal facies in Belgium and the southeast of the UK.

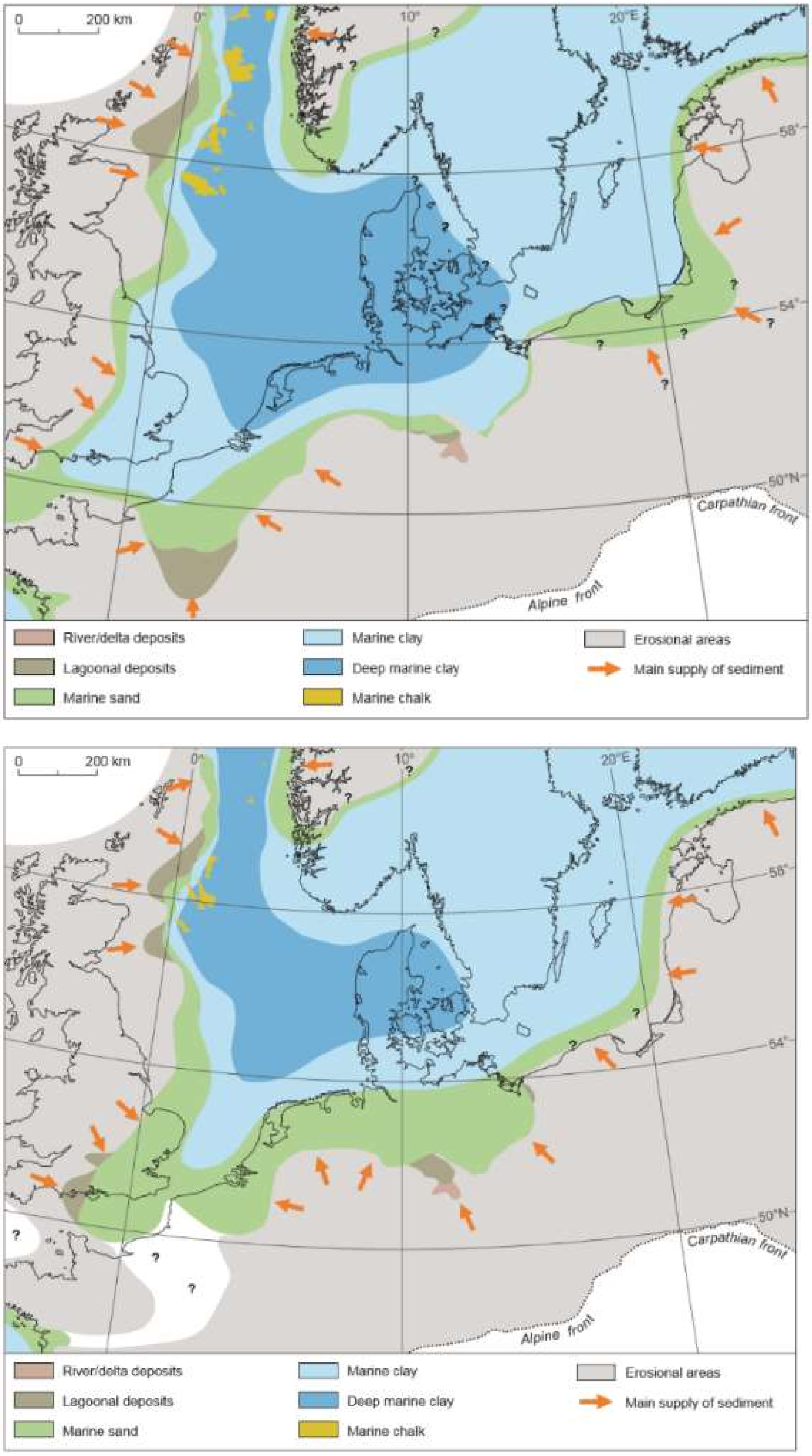

Figure 4-1 *Paleogeographic reconstructions and distribution of predominant sediment types in northwestern Europe for **(upper)** the Early Eocene (early Ypresian, deposition of the Ieper Mb.) and **(lower)** the Middle Eocene (early Lutetian, deposition of the BSM in green) situations. Adapted from Gibbard and Lewin (2016).*

4.2 Lithostratigraphic nomenclature

In terms of lithostratigraphy, the strata defining the BSM belong to the **Lower North Sea Group**, which in turn encompasses two Formations, the Paleocene **Landen Formation** and the Eocene **Dongen Formation**.

In the Dongen Formation various Members are recognized, some of which have a widespread distribution. Recently the official stratigraphic nomenclature of the Dongen Formation was modified. The names of the historically used Members that bear the term "Dongen" in them were modified. In the basal Eocene of the northern half of the Netherlands, tuffaceous volcanoclastics of the **Basal Dongen Tuffite Member** (recently renamed as **De Wijk Member**) are encountered. In the southern half of the Netherlands, shallow marine sand of the **Basal Dongen Sand Member** (recently renamed as the **Oosteind Member**) characterize the Lowermost Eocene. During the early Eocene (Ypresian stage), a substantial transgression led to the development of widespread clay deposition, the **Ieper Member**. Up-section this member is characterized by an increase in the frequency and thickness of sandy intercalations. This complicates the recognition of the base of the overlying **Brussels Sand Member** (from now on referred to as BSM), the sand-dominated unit that was mapped for the purpose of this study.

According to its original definition (Van Adrichem Boogaert and Kouwe, 1994), the BSM is "…*characterized as a succession of green-grey, glauconitic, very fine-grained sand with, mainly in the upper part, a number of hard, calcareous sandstone layers. Towards the base of the unit the clay content increases, and the calcium carbonate content and amount of glauconite decreases. A minor amount of mica occurs. Farther from the palaeo-coastline the member becomes silty and marly*." Note that the latter has led to the designation of the **Brussels Marl Member**, which is essentially recognized north of northernmost Friesland and Groningen. According to its original description, The BSM is of early Middle Eocene age (Ypresian to Lutetian Stage). However, this original description does account for the apparent identification of a series of unconformities and/or sequences in the BSM, as is depicted in the stratigraphic chart that accompanies the Nomenclator of the Netherlands (see Figure 3-2). From this diagram a picture emerges in which the BSM composes:

1. A lowermost (Ypresian-age) sequence that concordantly overlies the Ieper Mb.
2. A Lutetian sequence (or sequences), that unconformably overly the Ypresian part of the Member and underly the Bartonian or younger strata
3. In the southern part of the Netherlands, it is suggested that a sand-dominated upper Lutetian interval concordantly underlies the Lutetian-Bartonian claystones of the Asse Member.

The abovementioned **Asse Member**, with a late middle Eocene (Bartonian) to late Eocene (Priabonian) age, is the youngest of the members of Dongen Formation and consists of glauconite-containing plastic clay. Notably the upper part of the member is sandy and deposited in a more proximal setting.

The Oligocene to lowermost Miocene succession in the Netherlands belongs to the **Middle North Sea Group**. Of particular relevance for this study are the Lower Oligocene (Rupelian) units of the **Rupel Formation**. A stratigraphically complete succession through this formation is characterized by a basal (latest Eocene to lowermost Oligocene) sand-dominated interval, historically known as the **Vessem Member** (recently renamed as **Berg Member**). Subsequently, Lower Oligocene sediments are dominated by fine-grained deposits of the Rupel Clay Member (again, recently renamed as **Boom Member**).

The effects of uplift during the Pyrenean and Savian tectonic phases have strongly affected the thickness of sediments of the Dongen Formation. Often, the Oligocene strata of the Rupel Formation unconformably overly the Dongen Formation. This implies that the Asse Mb. and/or BSM are (partially) eroded.

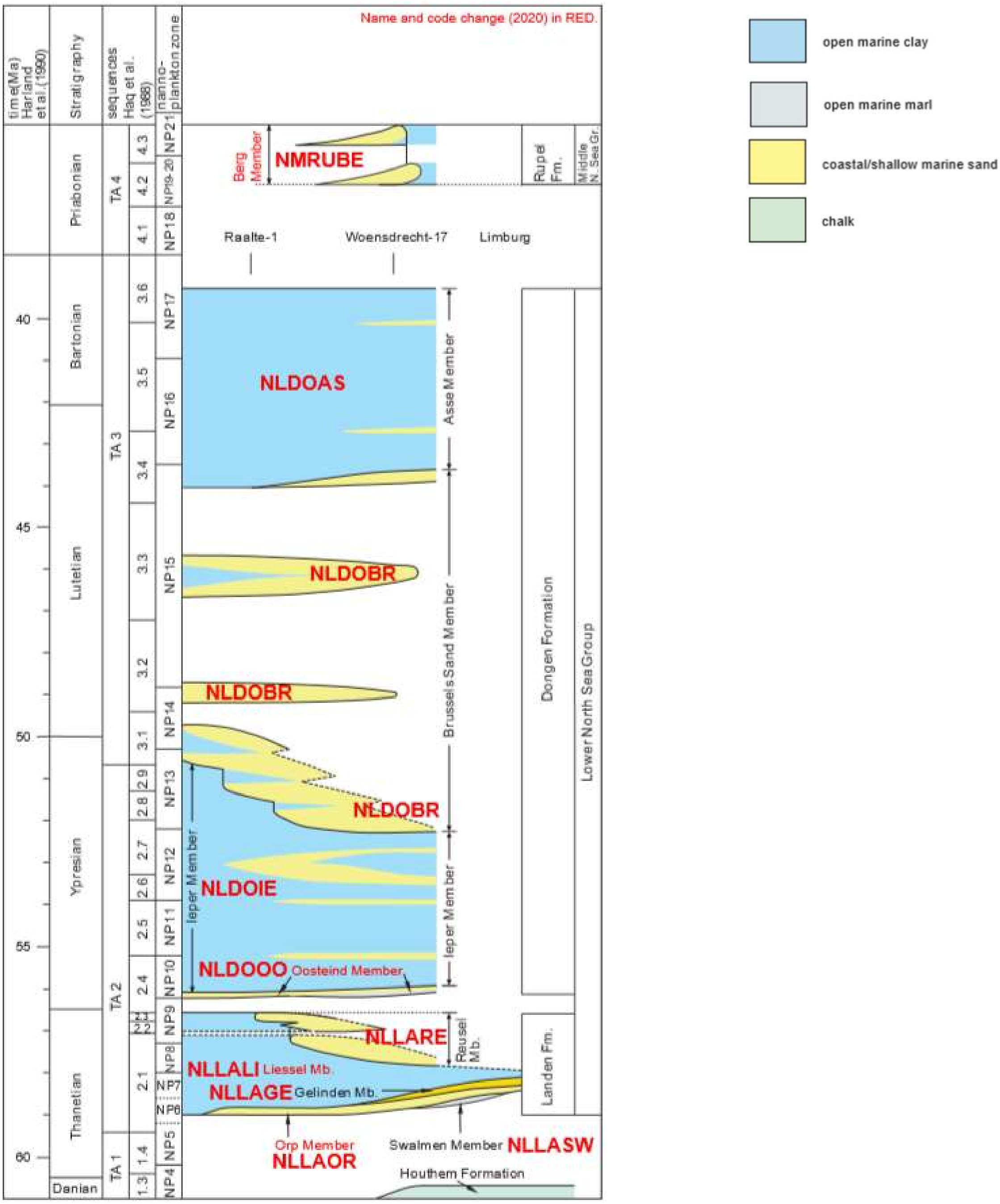

Figure 4-2 *Schematic stratigraphic diagram for the Paleocene-Eocene successions in the Netherlands. The abbreviations in red follow the most recent stratigraphic nomenclature. See* Table 4-1 *for the corresponding outdated nomenclature. Adapted from https://www.dinoloket.nl/stratigrafische-nomenclator/achtergrondinformatie/stratigrafische-tabellen*

In addition to the nomenclatural modifications of the Members of the Dongen and Rupel Formations, the abbreviations used by the Geological Survey of the Netherlands were also modified. For the sake of consistency with products currently used by the stakeholders of the project (e.g., ThermoGIS), we maintain the "old" abbreviations and terminology in this report. Table 4-1 presents an overview of the modifications.

Table 4-1 *Overview of modifications to the naming of lithostratigraphic units in the Eocene and Lower Oligocene stratigraphy of the Netherlands. The outdated nomenclature is indicated in red, the new in green. The former is used in this report for consistency with the ThermoGIS website.*

Group	Abbrev.	Formation	Old abbrev.	New abbrev.	Old Members	Old abbrev.	New Members	New abbrev.
Middle North Sea	NM	Rupel (Oligocene)	NMRF	NMRU	Rupel Clay	NMRFC	Boom	NMRUBO
					Vessem	NMRFV	Berg	NMRUBE
Lower North Sea	NL	Dongen (Eocene)	NLFF	NLDO	Asse	NLFFB	Asse	NLDOAS
					Brussels Marl	NLFFM	Brussel Marl	NLDOBM
					Brussels Sand	NLFFS	Brussel Sand	NLDOBR
					Ieper	NLFFY	Ieper	NLDOIE
					Dongen Clay	NLFFC	Engelschhoek	NLDOEN
					Basal Dongen Sand	NLFFD	Oosteind	NLDOOO
					Basal Dongen Tuffite	NLFFT	De Wijk	NLDOWY
		Landen (Paleocene)	NLLF	NLLA	Reusel	NLLFR	Reusel	NLLARE
					Landen Clay	NLLFC	Liessel	NLLALI
					Gelinden	NLLFG	Gelinden	NLLAGE
					Heers	NLLFS	Orp	NLLAOR
					Swalmen	NLLFL	Swalmen	NLLASW

4.3 Well log character and correlation

4.3.1 Stratigraphic well interpretation

Due to Oligocene-Miocene inversion during the Pyrenean tectonic phase, there is a clear subdivision in the distribution of the BSM, leading to the designation of a southern and a northern study area. For the southern study area, all wells from within and surrounding the distribution of the BSM as used for ThermoGIS 2.1 were selected for stratigraphic evaluation. For all these wells, wireline log data were collected. For interpretation the gamma ray (GR) and sonic (DT) logs were considered guiding. For vintage wells (e.g., from the 1940s-1950s) the spontaneous potential (SP) log was considered in absence of DT and GR logs. Well tops on three hierarchical levels (Groups, Formations, Member) were loaded. In a large number of wells, the interpreted stratigraphy was on Formation rather than on Member level, whereas the members of the Dongen Fm. could be clearly recognized on logs. Through the construction of numerous cross sections a three-partitioning of the BSM became evident in an early stage. This partitioning could be traced in most of the wells containing GR and DT log data (see Section 4.3.2). The wells having only an SP log turned out more difficult to correlate on this level of detail, particularly because only the top could be consistently correlated using the SP log. The BSM and its respective sequences were subsequently interpreted in 54 wells.
In the north of the study area the stratigraphic database from ThermoGIS 2.1 was taken as a starting point. In this database the BSM. was identified in 599 wells (incl. sidetracks). Due to this large number of wells, a full-scale re-interpretation of wells was deemed unrealistic. Therefore, a selection of wells displaying apparent bullseyes in the thickness of the BSM and wells along the distribution limit were re-evaluated in detail. If there turned out to be reason for reinterpretation this was accordingly done. In other cases, the quality of petrophysical logs was not sufficient for reliable stratigraphic interpretation. These wells were subsequently discarded. This pertains to a total of 153 out of the total 599 wells in the northern part of the study area.

4.3.2 Sequences in the Brussels Sand Mb.

In order to describe the trends from petrophysical log properties across the BSM, we here consider two characteristic wells; Brouwershavense Gat (BHG-01) and Kortgene (KTG-01). Both wells are from the western edge of the southern study area in Zeeland (Figure 4-4). Both wells contain a rather complete succession across the Dongen Formation, comprising the Ieper Member, the BSM and the Asse Mb.
The gamma-log profile of these wells displays three distinct “cleaning-up” cycles in association with the BSM (Figure 4-3). The lowermost cycle is referred to as Sequence 1, the more clayey zone near top of this sand-dominated interval is termed Sequence 1a. In sequence stratigraphic terms, it is more logical to consider the latter as the basal part of the overlying Sequence 2. Yet, in lithostratigraphic terms it is here maintained as part of Sequence 1. The gamma-log trends are in this case not simply a function of clay versus sand content, as the BSM. contains substantial amounts of glauconite and mica/muscovite. The high gamma streaks observed at the base of Sequence 3 and near the top of Sequence 3 are likely caused by accumulations of these minerals.
The sonic velocity (DT) profiles display the persistence of “fast” spikes, particularly in Sequence 3. These are interpreted as zones affected by carbonate-cementation. This has been recorded in lithology descriptions based on cuttings and the few available cored sections (e.g., AHO-E55 and DON-01) through the BSM. The sand-dominated intervals of Sequence 1 and 2 also display some “fast” streaks, in contrast to the underlying Ieper Mb. Yet, the conspicuous spikes seem restricted to Sequence 3.
Based on only these two wells it becomes immediately clear that the base of the BSM as provided by the lithostratigraphic interpretations database of the Geological Survey of the Netherlands (available through http://www.dinoloket.nl) is positioned above the base of Sequence 1 and

approximates the base of Sequence 2. However, if one considers the information provided by the Stratigraphic Nomenclator for the Netherlands (see Section 1.2 and Figure 2), the base of Sequence 1 (the first sandstone occurring in/above the Ieper Mb.) seems a more appropriate criterion for the base of BSM.
In a complete, non-truncated setting, the criteria for picking the top of the BSM are somewhat complicated, due to an offset in the behaviour of the gamma and sonic velocity logs. As illustrated by both wells, the gamma values increase substantially near the top of Sequence 3, whereas the sonic velocities remain high. This may be caused by the enrichment of glauconite/muscovite during the latest phase of sand-deposition of Sequence 3. The top of the BSM is most confidently picked if both GR (top of sand / muscovite) and DT (termination of spiky pattern) are available.

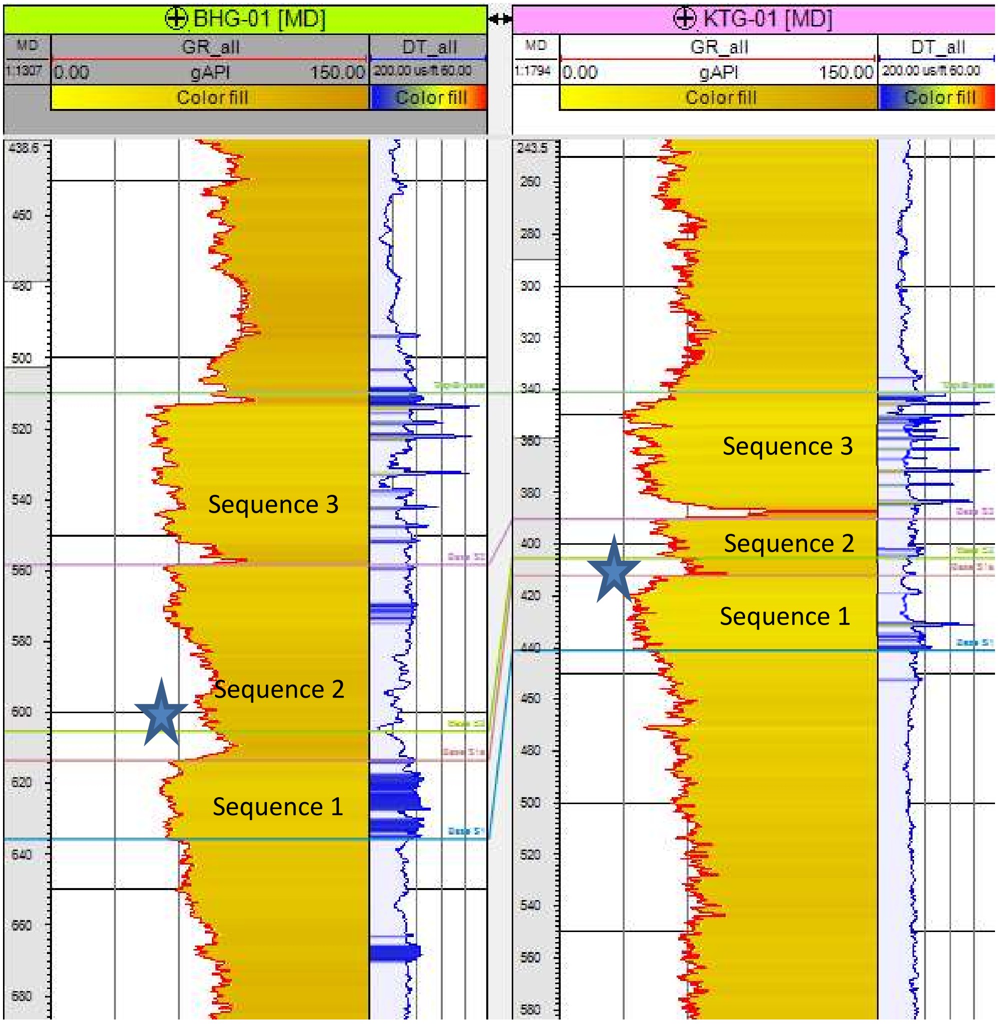

Figure 4-3 *Typical well-log section through the BSM in two wells from Zeeland (BHG-01 and KTG-01). The coloured horizontal lines indicate the delineations of the sequences recognized in this study. The blue stars indicate the base of the BSM according to the lithostratigraphic interpretation provided by the Dinoloket.nl website. It is clear that Sequence 1 is positioned below the interpretation provided by Dinoloket.nl.*

There is limited biostratigraphic data that could elucidate the respective age differences between these three sequences. In the southern study area, in well Hilvarenbeek (HVB-01) the BSM is only represented by Sequence 1. Here, it is immediately overlain by the Oligocene sandstones of the Vessem Mb. Munsterman and Kerstholt-Boegehold (2015) show that the Sequence 1 interval is of early Lutetian age. For the Waalwijk area, Munsterman (2017) shows that in wells Sprang (SPG-01), Waalwijk Noord (WWN-01) and Waalwijk (WWK-01), Sequence 1 is of a similar early Lutetian age. Here the BSM is unconformably overlain by the Rupelian age strata of the Rupel Clay Mb. Hence, based on the abovementioned biostratigraphic evidence, it seems that

Sequence 1 is consistently of early Lutetian age and that Sequence 3 is of late Lutetian age. This implies that the base of the BSM is not of Ypresian age as suggested by the Nomenclator of the Netherlands (see also Figure 3.2).
In the northern study area only three wells have biostratigraphic age-control (Raalte (RAL-01, Munsterman, 2002), Akkrum 3 (AKM-03, Munsterman, 2020a) and Zuidwal 2 (ZDW-02, Munsterman, 2020b). In these wells, the BSM is consistently characterized by palynological assemblages indicative of a middle-late Lutetian age. None of these studies have specifically sampled Sequence 1, 2 or 3. Nevertheless, there is no biostratigraphic evidence to infer an Ypresian age for Sequence 1.

4.3.3 Stratigraphic correlation panels

The following section presents a series of well-log correlation panels in order to (A) provide an overview of the stratigraphic development of the BSM and (B) to illustrate the differences between the original stratigraphic interpretation of Dinoloket. A short discussion of the main features and trends can be found in the respective figure captions. Figure 4-4 shows the location of the wells and transects.

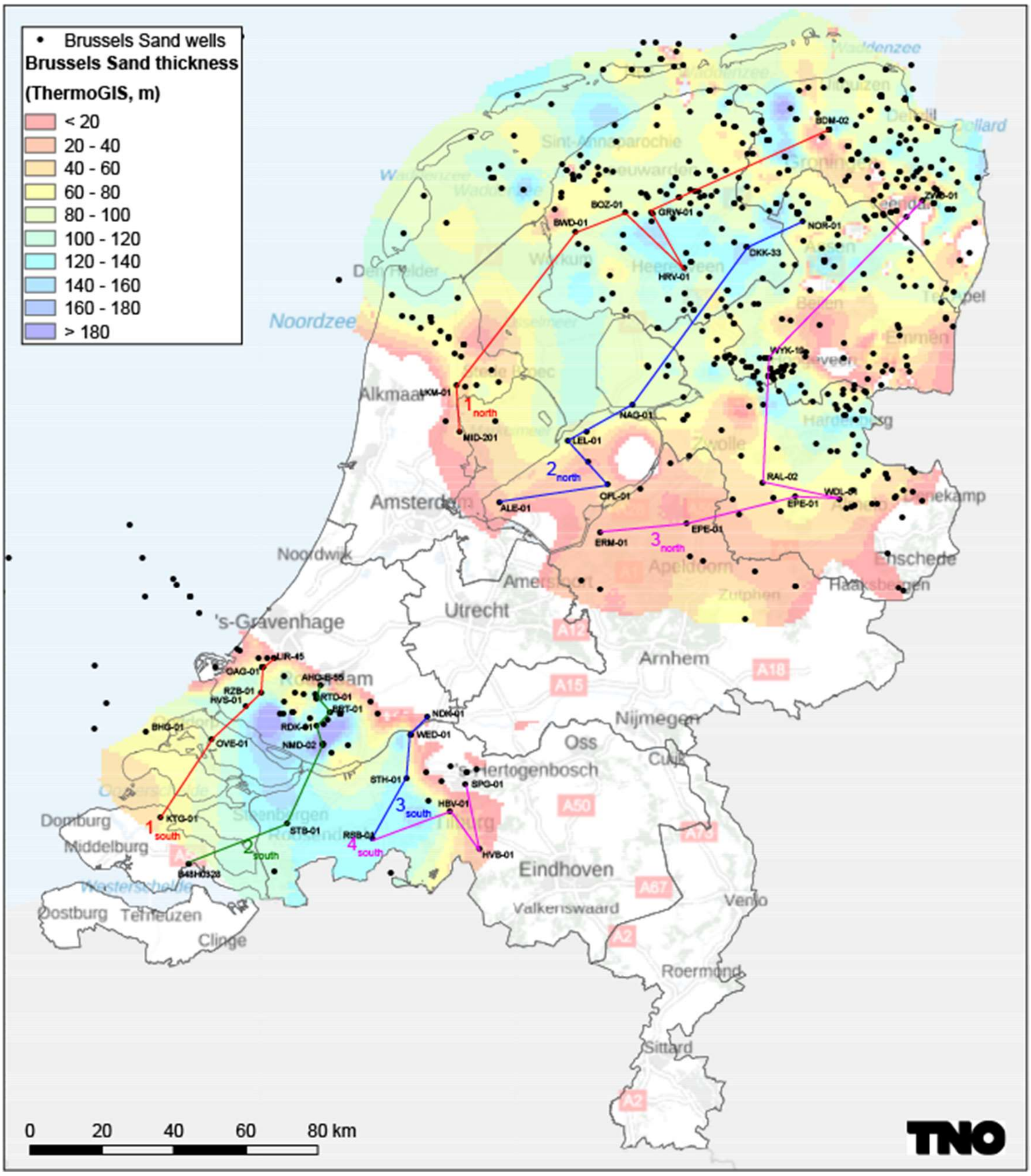

Figure 4-4 *Position of the four well-correlation panels in the southern study area and the three panels in the northern study area.* ***The basemap shows the thickness and distribution of the BSM according to ThermoGIS 2.1. The integrated results of the current project led to an update of this thickness map (see Appendix 3, Figure 9-4).***

Southern study area

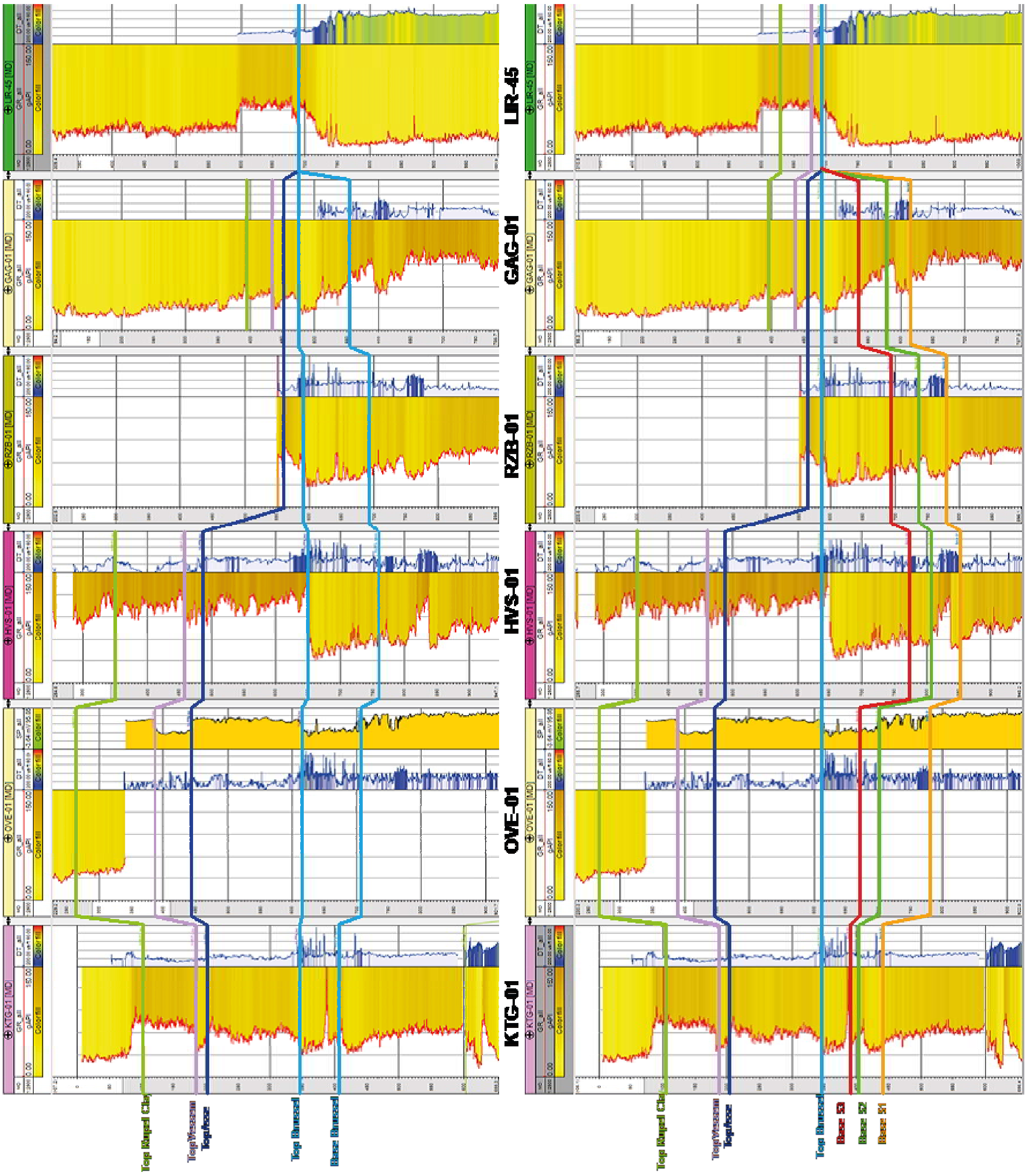

Figure 4-5 *Well section panel 1$_{south}$. GR and DT logs are plotted (see Figure 4-4 for well locations). For well OVE-01 also the SP log is available for the section that lacks a GR-log. The upper image displays the well markers according to the Dinoloket/ThermoGIS database. The lower image displays the new well marker interpretation, including that of the Brussel Sand Sequences. In essence, the base of the Brussel Sand sensu Dinoloket/ThermoGIS approximates the base of Sequence 2. Towards the north (GAG-01) the BSM seems to become stratigraphically thinner. Since the Asse Mb. here overlies the BSM, this is not a consequence of erosion into Sequence 3. In LIR-45 the BSM is eroded. Here the sand of the Vessem Mb. overlies the Ieper Mb.*

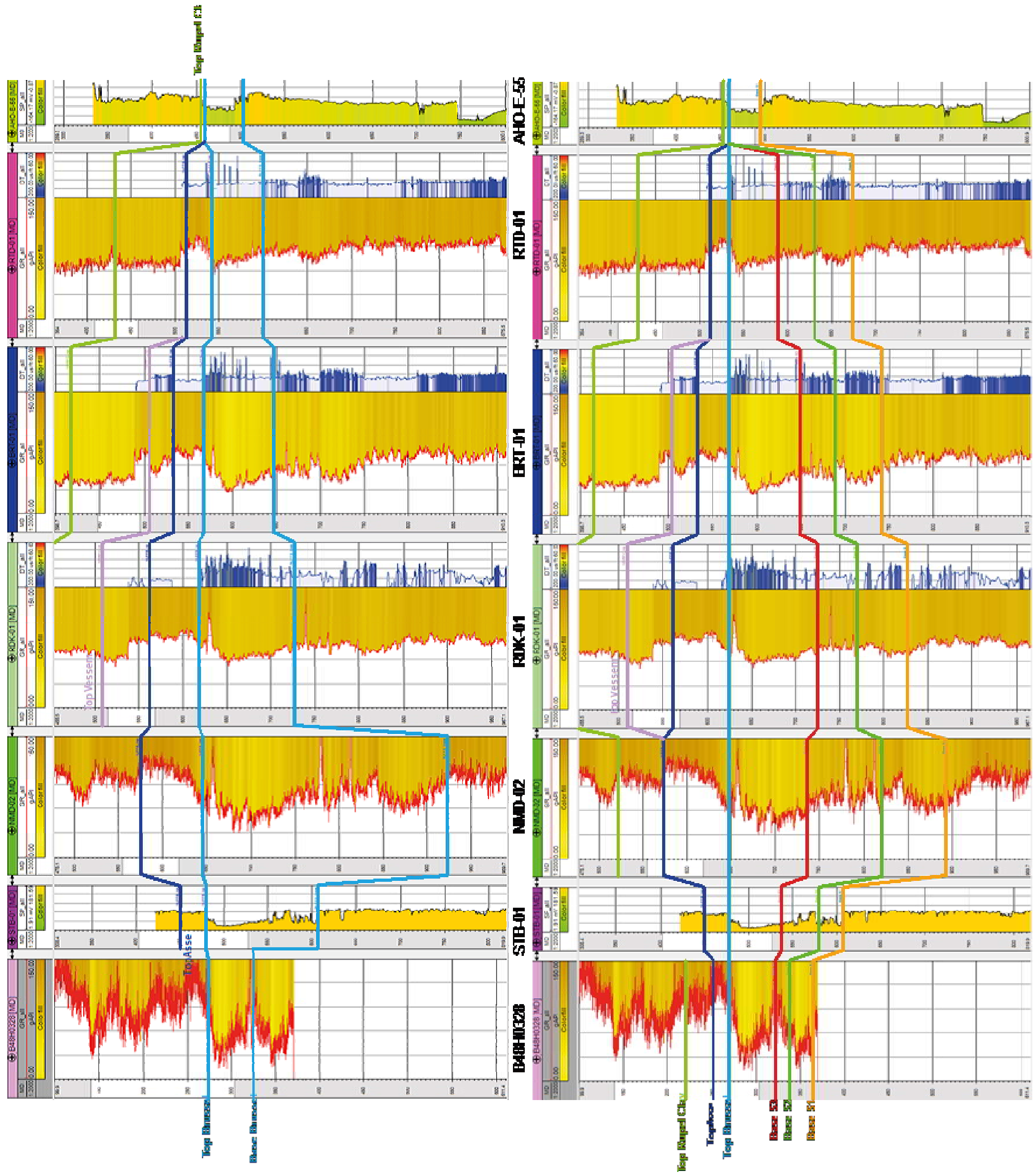

Figure 4-6 *Well section panel 2*$_{south}$*. GR and DT logs are plotted (see Figure 4-4 for well locations). Well B48H0328 is a shallow drillcore. For wells STB-01 and AHO-E55 only the SP log is available. The upper image displays the well markers according to the Dinoloket/ThermoGIS database. The lower image displays the new well marker interpretation, including that of the Brussel Sand Sequences. Note that for STB-01 and AHO-E-55 no interpretation on the sequence level was possible since the required logs were not available. In essence, the base of the Brussel Sand sensu Dinoloket/ThermoGIS approximates the base of Sequence 2. In a northward direction (wells RTD-01) the BSM first stratigraphically thins out, and in AHO-E-55, it is partially eroded by the Pyrenean unconformity. In well RTD-01, the Pyrenean unconformity cuts down into the Asse Mb. but not in de BSM. The Asse Mb. is immediately overlain by the Rupel Claystone Mb. The Vessem Mb. is absent. In well AHO-E-55 the Rupel Claystone Mb. immediately overlies the Brussel Sand Mb. It is impossible to tell what stratigraphic sequence of the BSM is preserved in AHO-E-55 but is likely only Sequence 1.*

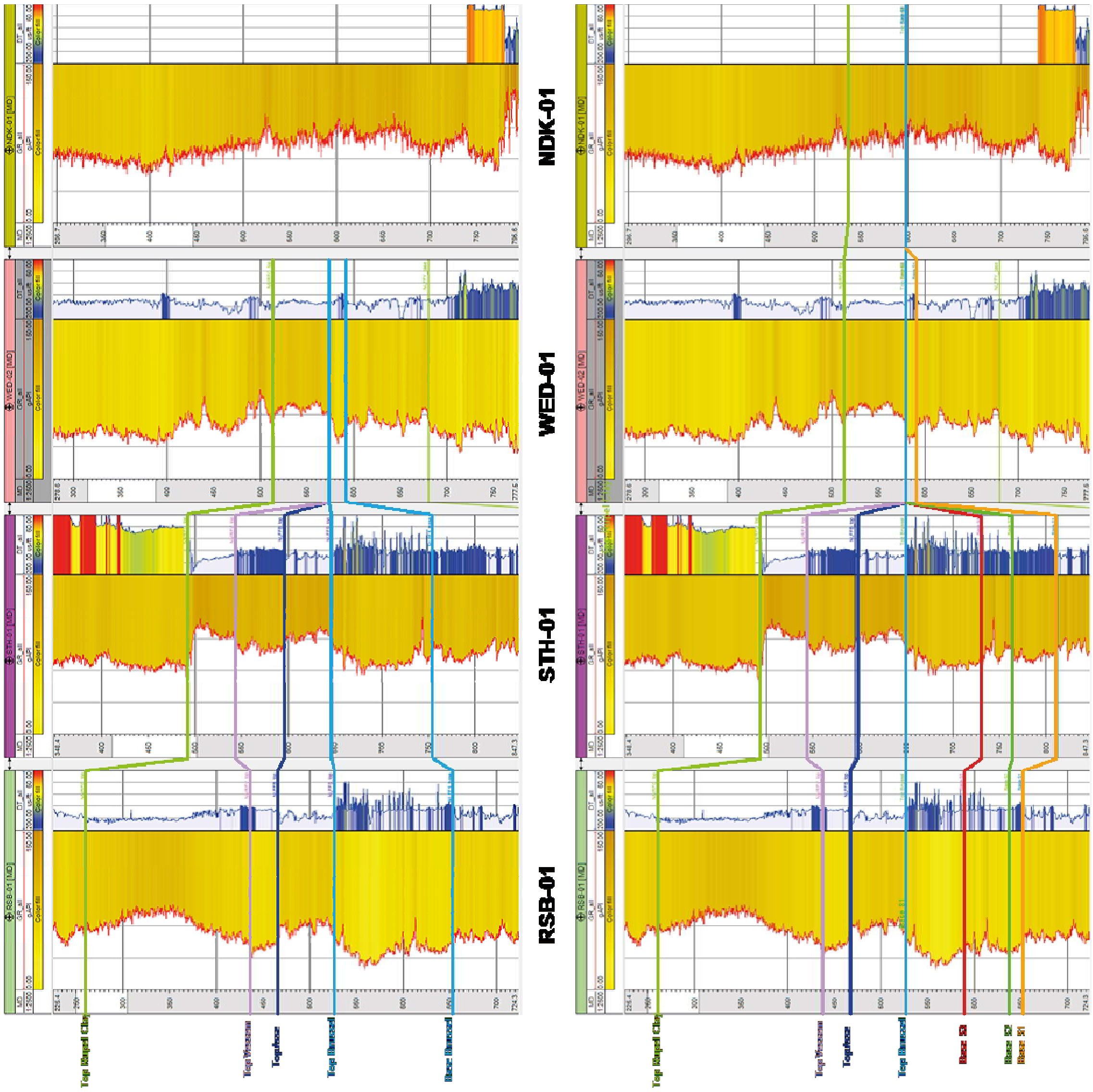

Figure 4-7 *Well section panel 3$_{south}$. GR and DT logs are plotted (see Figure 4-4 for well locations). The upper image displays the well markers according to the Dinoloket/ThermoGIS database. The lower image displays the new well marker interpretation, including that of the Brussel Sand Sequences. In essence, the base of the Brussel Sand sensu Dinoloket/ThermoGIS approximates the base of Sequence 2. This picture changes towards the inversion axis, where the Pyrenean unconformity cuts into the Brussel Sand Mb. beyond that level (i.e., into Sequence 1, see Well WED-01). In well NDK-01, a well that was initially only interpreted on Group-level, the Brussel Sand is completely eroded and the Ieper Mb. is overlain by the Rupel Clay Mb.*

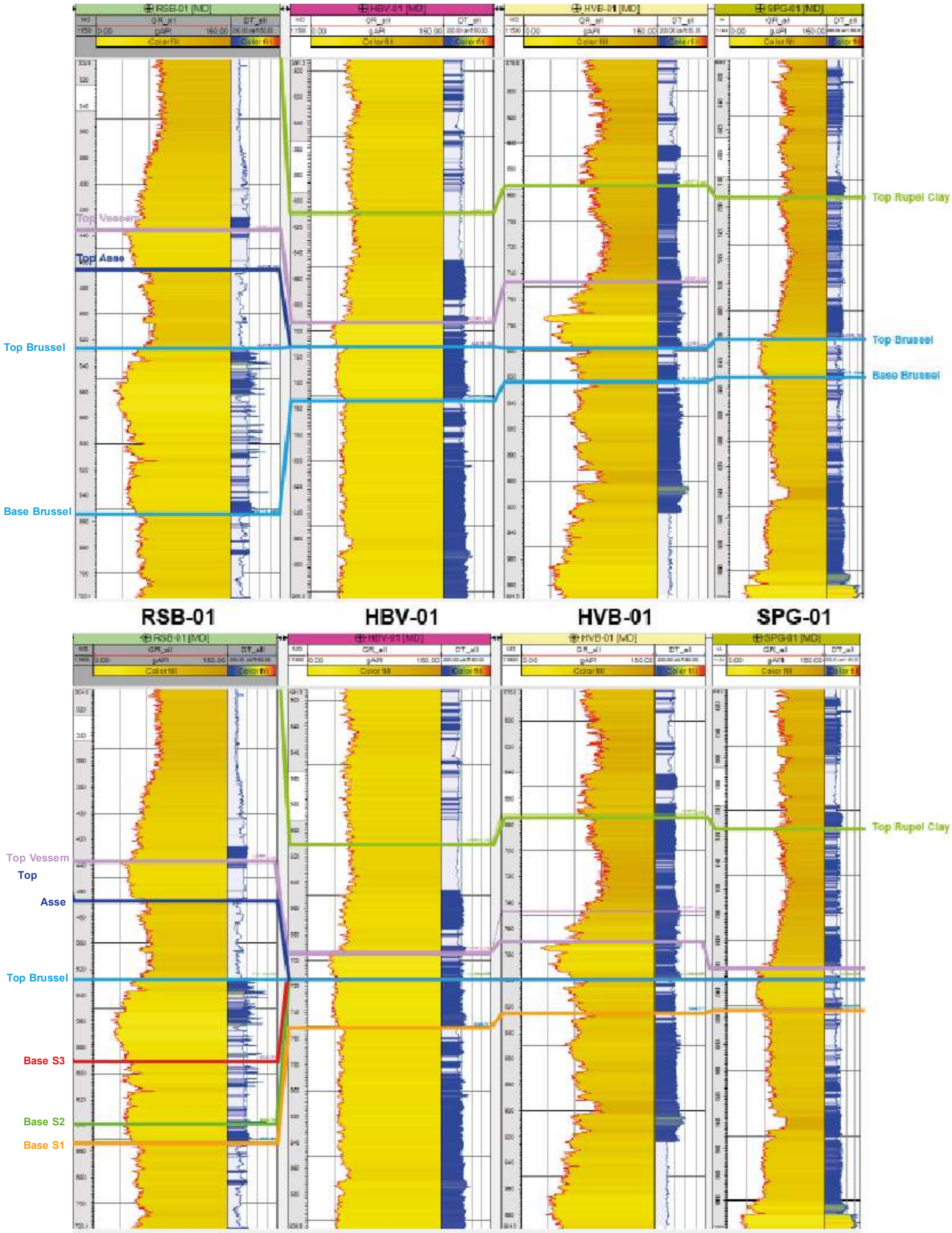

Figure 4-8 *Well section panel 4south. GR and DT logs are plotted (see Figure 4-4 for well locations). The upper image displays the well markers according to the Dinoloket/ThermoGIS database. The lower image displays the new well marker interpretation, including that of the Brussel Sand Sequences. In essence, the base of the Brussel Sand sensu Dinoloket/ThermoGIS approximates the base of Sequence 2. This picture changes towards the inversion axis, where the Pyrenean unconformity cuts into the Brussel Sand Mb. beyond that level (i.e., into Sequence 1, see Well HBV-01, HVB-01 and SPG-01). In wells HBV-01 and HVB-01 the Pyrenean unconformity led to a contact between two sandstone units; Vessem Mb. on top of BSM in well SPG-01 the Vessem appears very thin.*

Northern study area

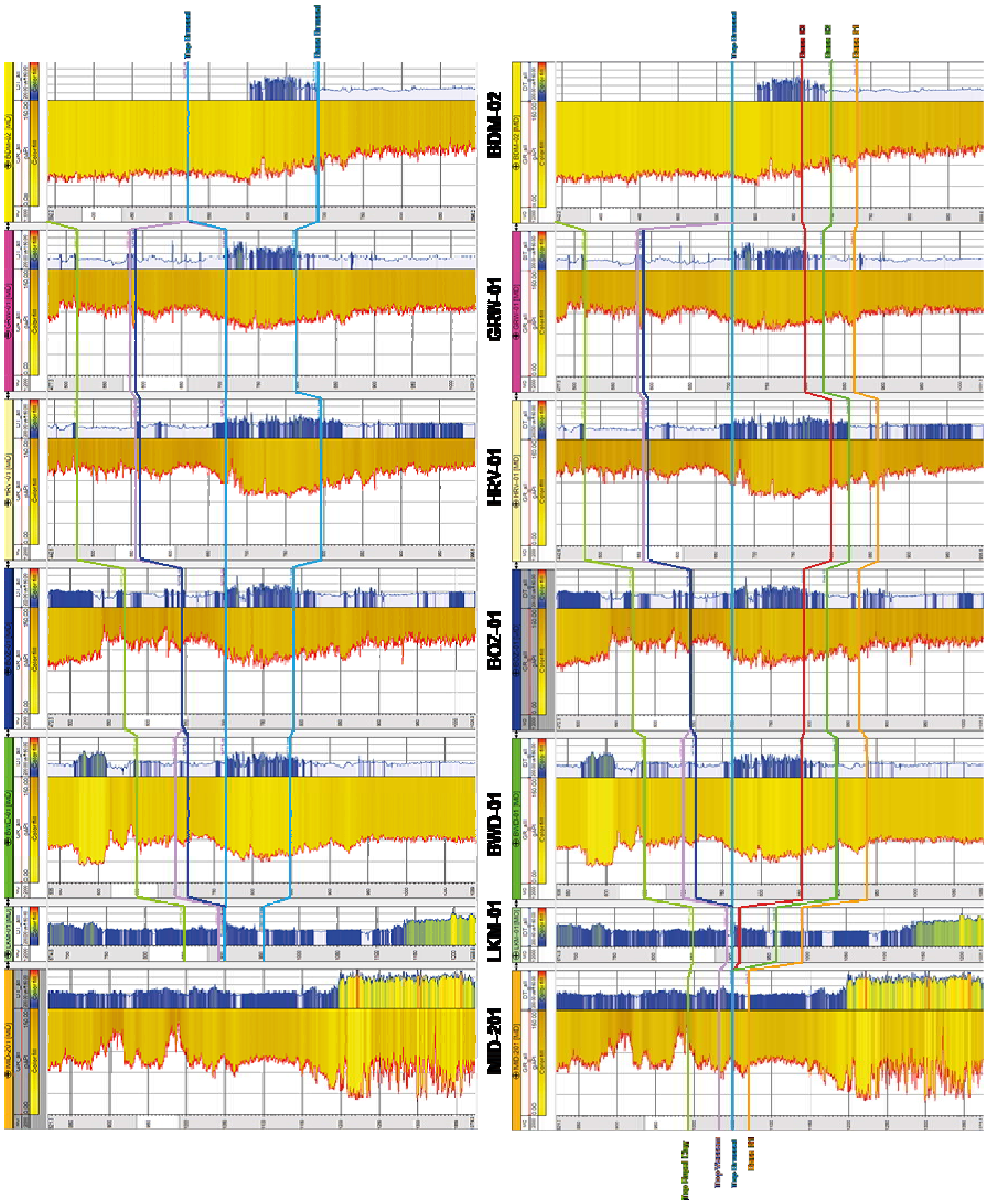

Figure 4-9 *Well section panel 1$_{north}$. GR and DT logs are plotted (see Figure 4-4 for well locations). The upper image displays the well markers according to the Dinoloket/ThermoGIS database. The lower image displays the new well marker interpretation, including that of the Brussel Sand Sequences. In essence, the base of the Brussel Sand sensu Dinoloket/ThermoGIS approximates the base of Sequence 2. Sequence 1 is developed quite clearly, yet never picked as the base BSM. The only exception is MID-201 (well had no initial stratigraphic interpretation) located close to the northern rim of the inversion axis. In well BDM-02, the top of BSM was picked erroneously in the Dinoloket stratigraphy.*

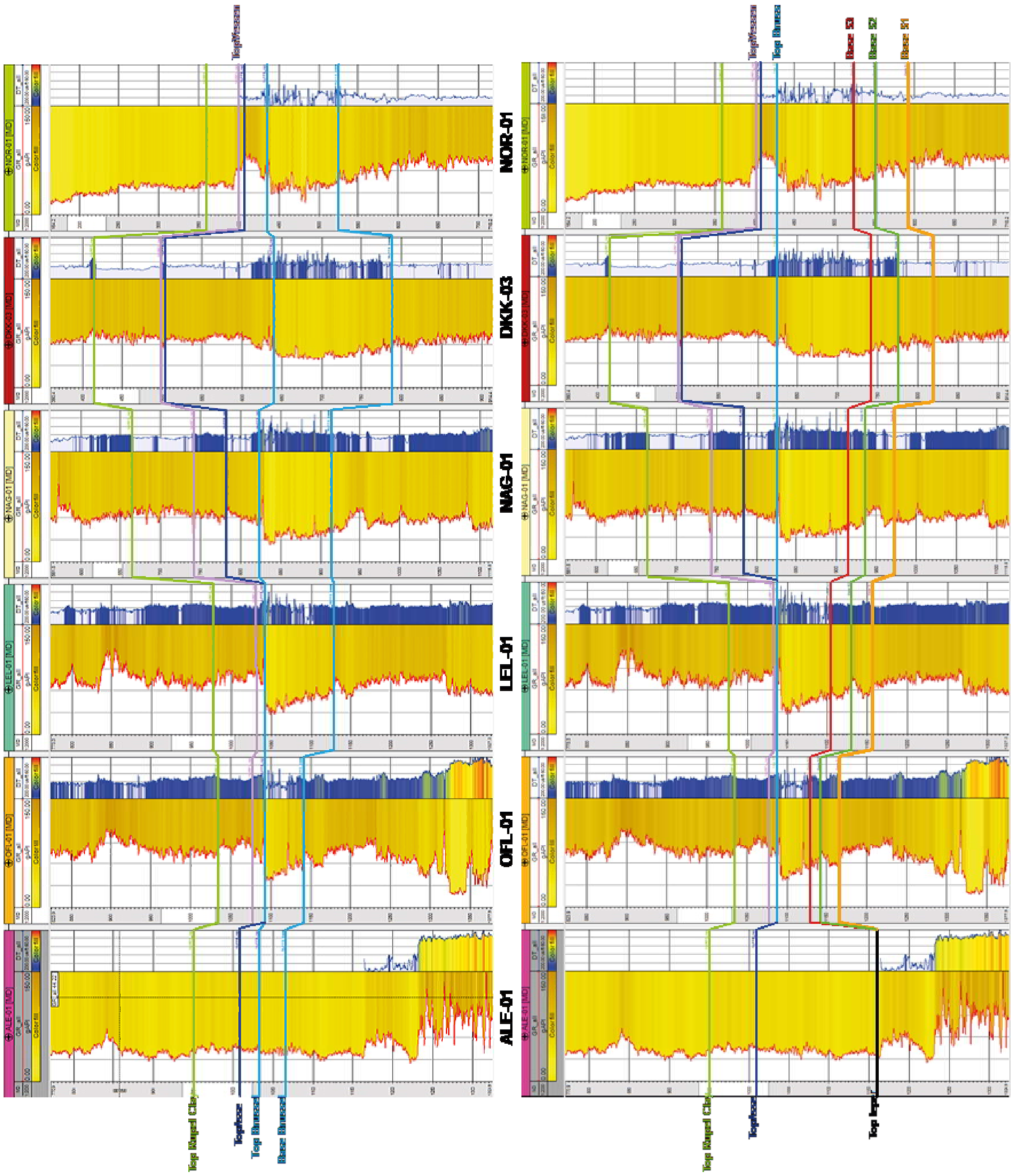

Figure 4-10 *Well section panel 2$_{north}$. GR and DT logs are plotted (see Figure 4-4 for well locations). The upper image displays the well markers according to the Dinoloket/ThermoGIS database. The lower image displays the new well marker interpretation, including that of the Brussel Sand Sequences. In essence, the base of the Brussel Sand sensu Dinoloket/ThermoGIS approximates the base of Sequence 2. In well ALE-01 the BSM is absent, in contrast to the Dinoloket/ThermoGIS interpretation.*

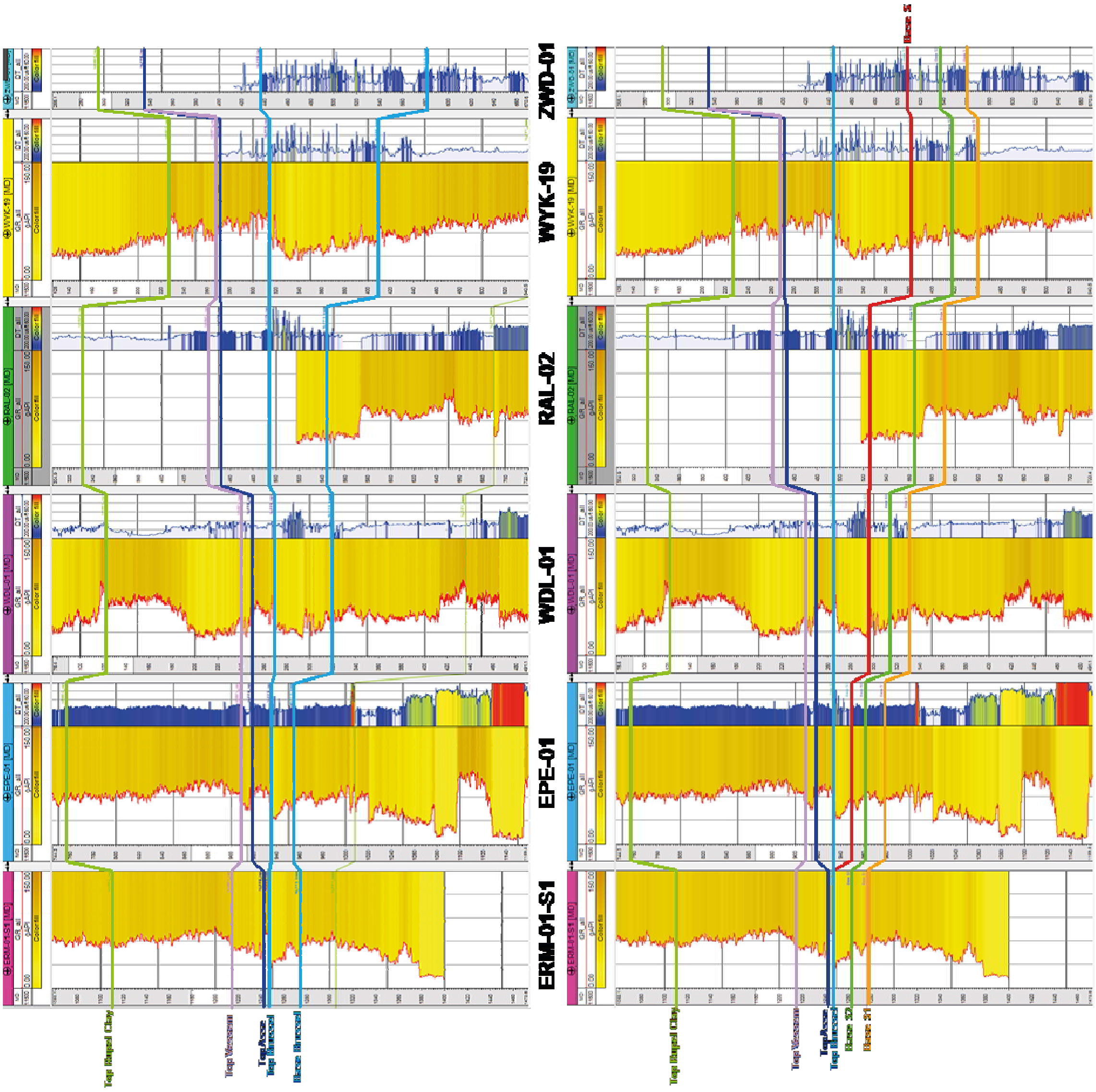

Figure 4-11 *Well section panel 2north. GR and DT logs are plotted (see Figure 4-4 for well locations). The upper image displays the well markers according to the Dinoloket/ThermoGIS database. The lower image displays the new well marker interpretation, including that of the Brussel Sand Sequences. In essence, the base of the Brussel Sand sensu Dinoloket/ThermoGIS approximates the base of Sequence 2.*

4.3.4 Well-top database and important deviations from the prior stratigraphic interpretation

Shallow wells

In ThermoGIS 2.1 and the stratigraphic database of dinoloket.nl, only interpretations (picks) for the BSM are included for 'deep' wells, typically drilled for hydrocarbon exploration and development or geothermal purposes. There are however also numerous 'shallow' wells that penetrate up to a depth of about 400 m. Often these wells were drilled for hydrological purposes. These wells are not routinely subjected to wireline logging and also the lithological sampling (cuttings) is often a very low resolution. Hence, they have a fairly high degree of stratigraphic uncertainty. Since in some parts of the two study areas (Zeeland in the southern study area and Twente in the northern study area), the BSM is found at very shallow depth (<500 m). In order to be able to provide realistic patterns in the distribution and approximate thickness, a number of these shallow wells were included (Figure 4-12). The stratigraphic interpretation essentially follows that of the hydrogeological Regis[1] model. In the Zeeland area, three wells reach beyond the actual base of the BMS (e.g., into the Ieper Mb.) and have sufficient quality GR-log data available to allow for recognition of the three sequences.

Figure 4-12 *So-called shallow wells that have recorded the BMS according to the REGIS Model. Note that about half of them terminates in the BMS and does not reach the base of the Member.*

Southern area:
In the southern study area, the BSM was interpreted in 89 wells (including sidetracks) which were used in ThermoGIS 2.1. For these wells, we evaluated if the available petrophysical logs were suitable. If so, the markers for Sequence 1-3 were interpreted. In addition, the stratigraphic interpretation of all wells located relatively close to the northern and eastern limits of the distribution of the BSM following ThermoGIS were checked. If necessary, the sequences 1-3 were (re-)interpreted. This resulted in 48 wells in which the Sequences 1-3 and the top of BSM were interpreted. Important deviations from the ThermoGIS 2.1 well-database include:

1. The BSM is present in the northwestern edge of the southern study area, near the Maasvlakte and 's Gravenzande. Wells MSV-01 and SGZ-01 were not included in the ThermoGIS mapping.
2. Wells in the Numansdorp area were erroneously thick in ThermoGIS because the base of the BSM was correctly placed at the base of what is herein termed Sequence 1, whereas in other wells the base of Sequence 2 was used. Now this former level is interpreted for all wells in the area. Therefore, the obvious bull's-eyes in the thickness map no longer exist.
3. Newly included wells in the Zeeland extend the distribution of the BSM to the southwest.
4. In the Waalwijk area, we identified a number of wells that have a thin Sequence 1 section through the BSM This led to modification of the distribution of the BSM in this part of the study area (see also Section 6).

Northern area:
For the northern study area, the number of wells is too high to allow for a full reinterpretation (599 wells, incl. sidetracks). However, the problem of the different criteria for the base of the BSM in the southern area (e.g., Sequence 1 vs. Sequence 2) is not an issue since an initial screening revealed a consistent pick of the base of Sequence 2 as the base of BSM (see also Figure 4-9 - Figure 4-11). More problematic is that in a large number of wells the wireline logs were strongly compromised by being run through casings and/or with contaminated drilling mud. Therefore, many initial lithostratigraphic interpretations, often copied directly from the completion logs, are deemed uncertain. Therefore, we have evaluated the well-logs from wells that cause obvious bull's-eyes in the ThermoGIS 2.1 maps. In some cases, these were caused by disputable interpretation of a sound well log. In those instances, the respective well markers were modified (depths marked in red in digital appendix 1). If the well logs are insufficient for interpretation they were marked accordingly in the well marker database and not further used for mapping purposes (see digital appendix 1). Out of 599 wells, 446 were considered to have reliable stratigraphic interpretations, some after modification.

A few important observations are that:

1. The southern rim of the distribution as proposed by ThermoGIS 2.1 is largely correct. An exception is well ALE-01 that has no characteristic signature of the BSM.
2. If preserved completely, the overall thicknesses do not vary greatly. The BSM in the northern study area is typically between 80 and 110 m thick (Base Sequence 2 considered as the base). A full reinterpretation with a consistent pick of Sequence 1 was not performed, also because the base of Sequence 1 is often difficult to recognize on seismics (see also Section 4.2.2.). If Sequence 1 would be included this would add approximately 30 m to the thickness.
3. The BSM seems to become muddier/marly towards the north. This is particularly clear in a few wells from the Wadden Sea area. It is sometimes difficult to differentiate between what would be interpreted as BSM and Brussels Marl Mb.

Digital appendix 1 provides a database of all well markers used in this study. For the northern study area, the appendix contains the updated tops and bases of the BSM (sensu Sequence 2) and an indication as to whether the well has a confident interpretation. For the southern study area, it includes all wells that drilled the BSM and have with suitable logs. are were interpreted in terms of the three sequences.

5 Seismic interpretation and well tie

5.1 Seismic data

All publicly released seismic data, consisting of 3D and 2D seismic data, was available for this study. The interpreted seismic data are displayed in Figure 5-1. For the Southwestern part of the Netherlands all 3D data and almost all 2D seismic lines were interpreted. For the Northern part of the Netherlands the 3D surveys and a selection of 2D lines, based on quality of the lines and regional coverage, was interpreted .

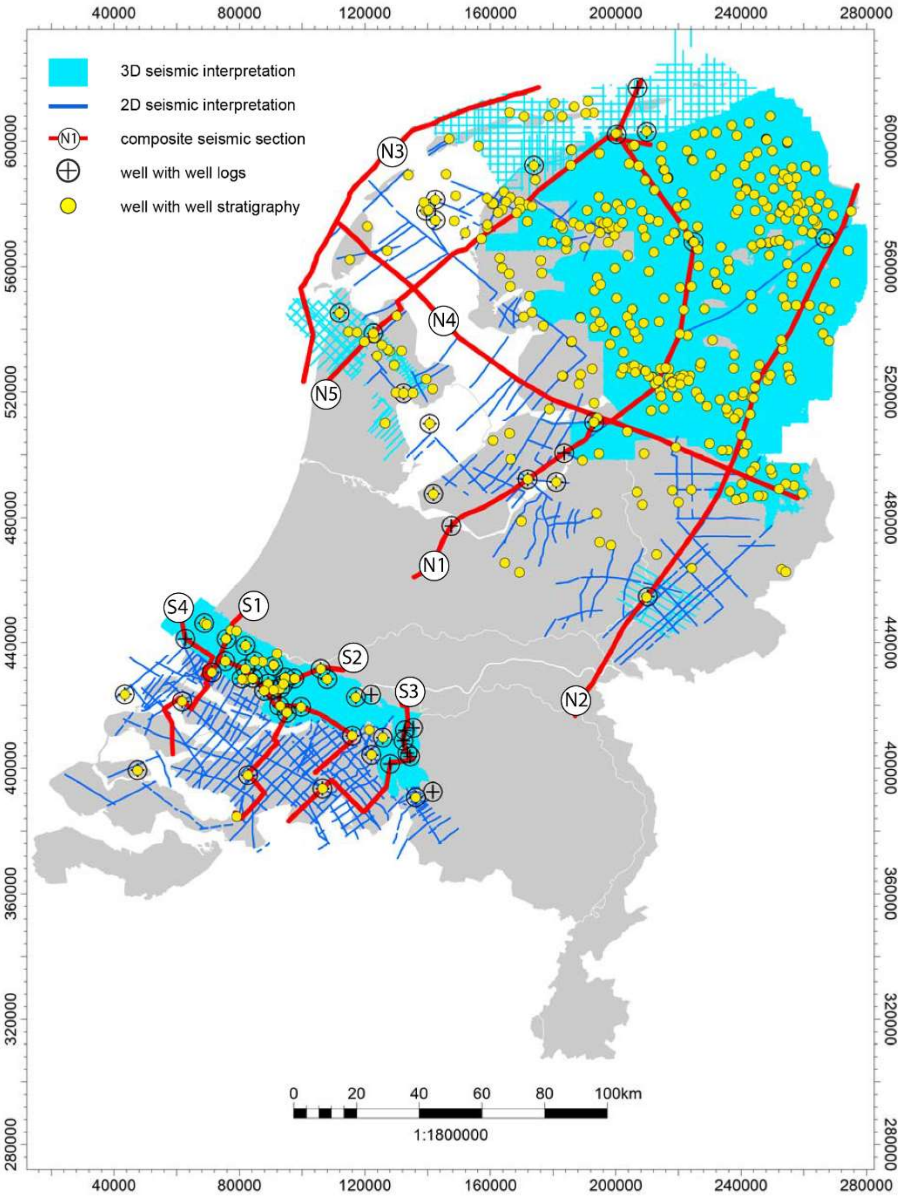

Figure 5-1: Interpretation and data coverage of the Northern and Southern study areas. Nearly half of the area where the BSM is present is covered by 3D seismic data. Used wells in yellow. The red lines are the composite seismic sections that are presented in Appendix 4. Along these sections a selection of wells and well logs the BSMis correlated in the well log panels displayed in paragraph 4.3.3.

The 3D surveys were all considered to be zero phase and shifted to the same polarity, resulting in troughs (negative numbers) corresponding to impedance increases. Determination of the phase of the 2D data is problematic. On some surveys/lines a phase rotation of 180 degrees has been applied to ensure more consistent seismic picking. Although probably some of the 2D surveys are minimum phase, no 90-degree shifts were applied since most of the surveys carried no information on the phase of the data.

The acquisition and processing workflow of the several vintages of seismic data is very different, resulting in a wide variety in frequency content and hence seismic resolution. Furthermore, there are static differences between surveys and the 2D migration results in mis-ties on crossing lines. These issues cannot be resolved for such a large dataset and will therefore have an impact on the accuracy of the seismic interpretation. This is discussed in paragraph 5.2.3.

5.2 Interpreting BSM on seismic

5.2.1 Well tie/synthetics

Several synthetic seismograms of wells have been made to understand the seismic signature at the top and the base of the BSM. The Paleogene section was often only logged with limited wireline log tools since the target of most wells was deeper. The top of the BSM can be picked with confidence on gamma ray (GR) logs showing higher GR values in the overlying Asse shales and lower GR values in the BSM (chapter 4). Sonic logs were only acquired in a small selection of wells. Density logs are even scarcer. On sonic logs that are available the BSM shows a velocity that is slightly higher than the overlying Asse and the underlying Ieper shales. This is mainly caused by cemented zones in the sandy intervals. Especially in cycle 3 (Chapter 4) there are thin zones of high compressional velocity that show up as spikes in the sonic log. The distribution of these cemented zones is quite erratic and below seismic resolution. It is likely that the seismic facies is reflective but varying laterally as a result of interference of reflected waves on these thin streaks interfaces, like the seismic character of the interval with thin coals in the Westphalian Coal Measures (Maurits Formation) described in Schroot & de Haan (2003). The top of the BSM that is expected to be an impedance increase does not always coincide with the minimum amplitude of a trough. Moreover, Figure 5-2 shows that there is not always a velocity break at the depth where the GR shows the break. The majority of wells indicate that there is a velocity increase close to the top Brussel justifying a trough to be picked on the chosen polarity of the seismic data. In part of the seismic data in the Southwestern part of the Netherlands the underlying peak was dominant and tracked with higher confidence (evident from composed sections in Appendix 2). This interpretation was later on shifted 13 milli-seconds (ms) (upward) to align with the trough picked elsewhere.

The Base of the BSM is less distinct on GR logs, because the lower part of the BSM is shalier than the upper part and grades into the Ieper. Based on regional significance and correlatability in Southwest Netherlands a trough was chosen that, after close correlation with well logs, turned to be an intra S1 event. In the modelling workflow (paragraph 6.1) this event was shifted downward (27 meter) to align with the base of the S1 cycle.

In the Northern part of the study area a dominant seismic peak was interpreted that is positioned at the base of the S2 sands (imaging the transition to lower velocity clay in between S2 and S1). This peak is therefore referred to as the near base S2. During the modelling workflow, a later shift of +10 meter was applied to better align with the base of S2 in well data. This seismic-to-well tie is consistent with existing seismic interpretations of the 3D seismic data that represent the former lithostratigraphic base of the BSM (i.e., the NLFFS level that corresponds to the base S2, see Chapter 3). The synthetic seismograms shown in Figure 5-2 and Figure 5-3 illustrate the well tie with seismic data.

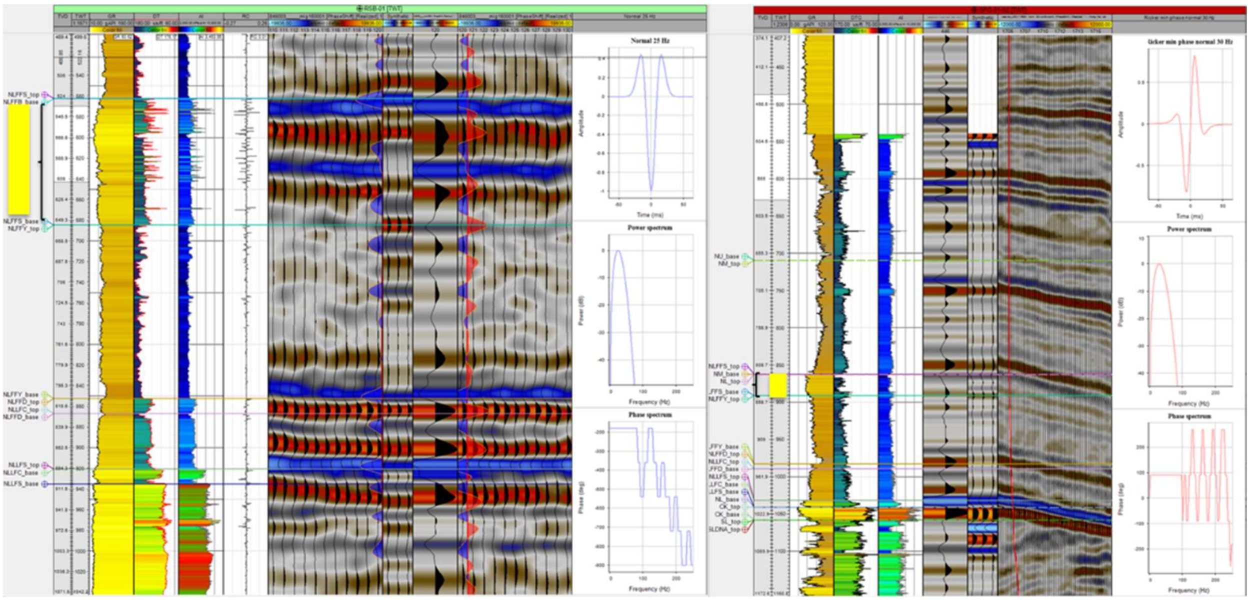

Figure 5-2 Synthetics for wells RSB-01 (left) and SPG-01-S2 (right).First panel Gr, second Sonic, third Acoustic Impedance. The synthetic traces are plotted in between the actual seismic data. In RSB-01 the BSM (indicated by the yellow bar) is relatively thick and has a reflective seismic facies corresponding with a spiky interval in the sonic log. In SPG-01-S2 the top of the BSM is eroded by the Rupel Formation and has lost the spiky interval in the sonic. Both wells show that base BSM is not a clear seismic reflector on the seismic data. While the top Brussel shows a positive impedance contrast in RSB-01, it shows a negative one in SPG-01-S2.

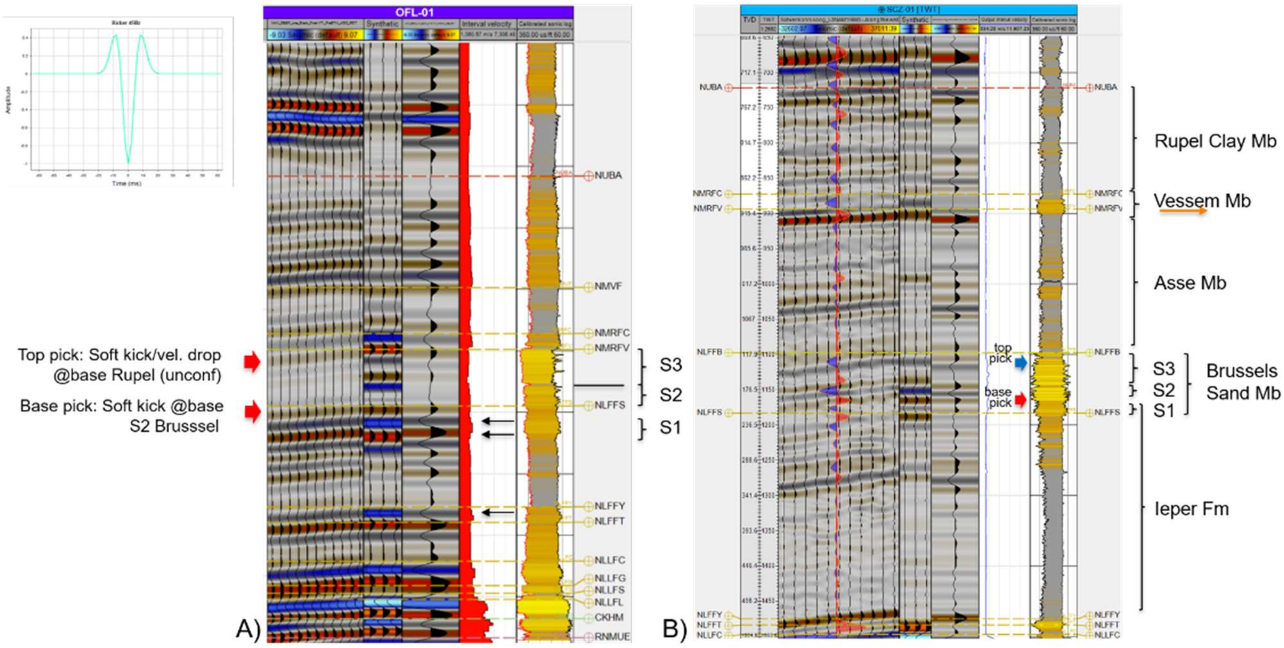

Figure 5-3 Seismic-to-well tie (synthetics) for two wells in the northern study area. A) well OFL-01, located in a domain where the BSM is uncomfortably overlain by the Rupel Formation. B) well SCZ-01, located further north, where the BSM is overlain by the Asse Member. In both wells the sonic velocity- and density logs were used to generate a synthetic seismogram using a 45 Hz zero phase, negative polarity Ricker wavelet (inset). The synthetic seismogram (2nd trace from the left) is compared to the seismic vintage used for interpretation (1st and 3rd trace show a sample of the seismic data and an amplitude log at well location) to select the best fit base and top pick for the BSM.

The BSM is directly overlain by the Rupel Formation (locally by its Vessem Member) where the overlying Asse clay and the upper part of the BSM were eroded during the Pyrenean inversion,. Here the separating unconformity is interpreted as well (Figure 5-4, Figure 5-5, Figure 5-6, Figure 5-7). The acoustic impedance contrast along the unconformity itself is varying by nature. Based on the seismic character at places where an angular unconformity is visible (truncation of seismic reflectors as in Figure 5-6) a peak was chosen to be interpreted. In the northern study area, the unconformity is represented as a peak (almost) everywhere. On the flanks of the WNW-ESE trending central Netherlands High, the Rupel Formation is eroded during the younger Savian inversion phase. Here the BSM is overlain by the Breda Formation.

5.2.2 Seismic interpretation and observations

After establishing a seismic-to-well tie, the applicability of the concept was tested by constructing regional seismic composites that cross the individual study areas both parallel and perpendicular to the main structural trend, i.e. SE-NW and SW-NE, respectively (Appendix 2). These composites confirm that the deposition of the BSM was continuous over a large area and its thickness was only locally affected by fault movement and salt doming. The present-day thickness is largely controlled by an inversion ridge that runs in a WNW-ESE direction over the central part of the Netherlands. Towards this high the BSM thins gradually and is eroded at both its NE (Figure 5-4) and SW flanks (Figure 5-5). While the area of thinning on the SW flank is covered by 3D seismic data, giving more certainty on the exact location of the pinch out it, is covered only by scarce 2D lines at the NE flank, with the exception of the province of North Holland where 3D seismic data is available (Figure 5-1).

In the southern area, no evident thickness changes can be observed over faults indicating that there was little or no fault activity during deposition. However, in the NE part of the Netherlands fault-block tilting and salt doming (Figure 5-7) caused local thinning and erosion of the BSM, suggesting that these processes occurred both during and after deposition of the BSM.
In the eastern part of the northern occurrence, along the Gronau fault zone, the structuration is rather complex. The BSM, Asse Member and Rupel Formation rapidly thin and shallow toward the fault zone and are truncated by the Upper North Sea Group deposits (see composite line N4 in Appendix 2). A number of shallow wells in this area provide some more insight into the distribution of the BSM.
Towards the southwest the BSM thins in a southward direction onto the London-Brabant Massif. It is buried shallowly or eroded. This is witnessed by shallow wells in the SW of the Netherland

(SW Zeeland). Unfortunately, no seismic lines are available in this shallow realm to study this thinning in detail.

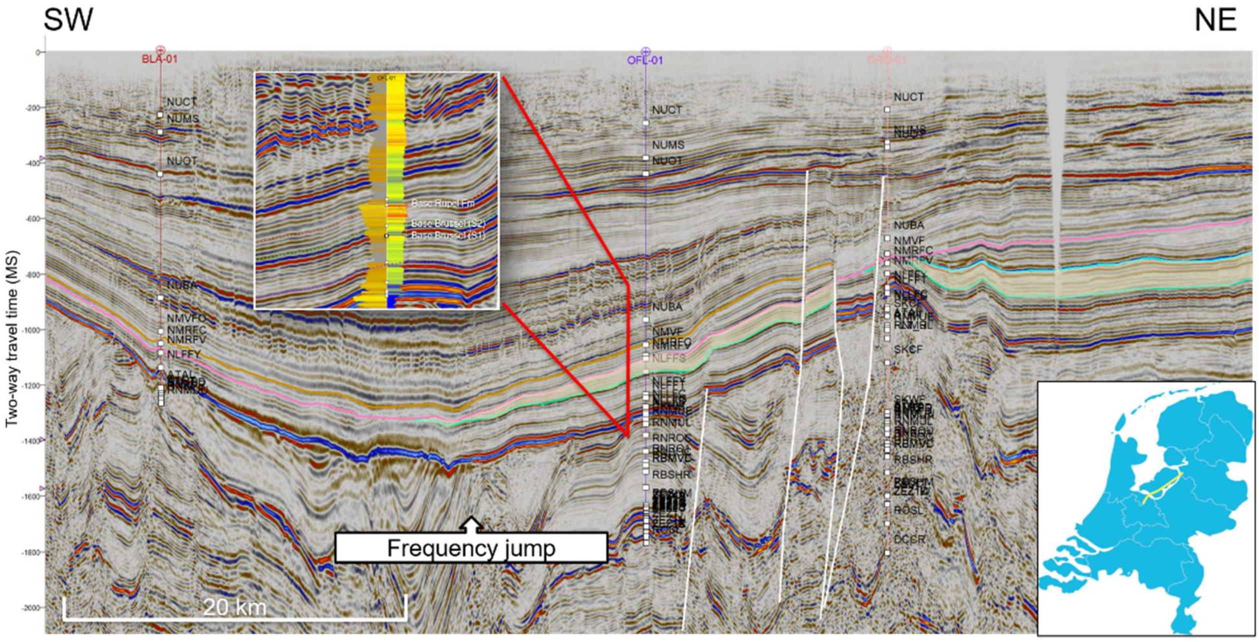

Figure 5-4 Composite seismic section including wells BLA-01, OFL-01 and DRO-01 (see inset for locality). The section shows the various scenarios for the occurrence of the BSM as discussed in the text. All horizons are bases. At BLA-01, the BSM (light green) is absent, at OFL-01 it is unconformably overlain by the Rupel Formation (pink); at DRO-01 it is absent due to erosion associated with local fault-block tilting and further north it is conformably overlain by the Asse Member (light blue). Upper-left inset show a detail of the seismic expression at well OFL-01, shown with a Gamma-Ray log indicating sand (yellow) and clay intervals (grey) and sonic velocity log (blue is low velocity, red is high velocity). Note that the BSM is thinning against the Dronten fault block (and later eroded and overlain by the Rupel Formation), suggesting syn-tectonic deposition.

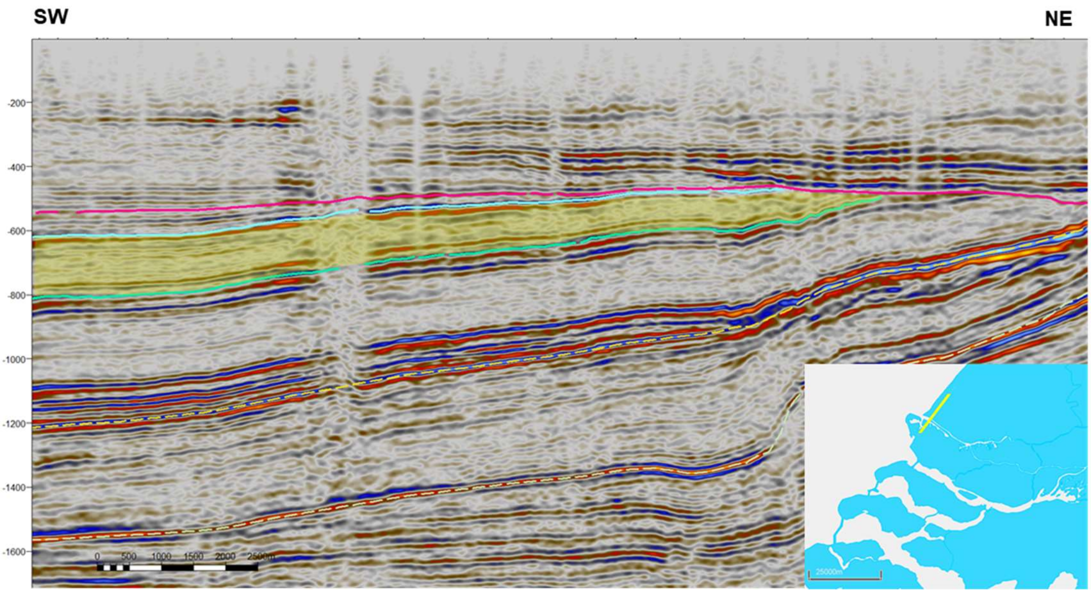

Figure 5-5 Seismic section from the 3D Monster survey showing the pinch-out geometry of the BSM caused by erosion of the top by the Rupel and Breda Formations (pink). Top BSM in light blue and the base in light green. Dotted lines represent base North Sea Group (yellow) and base Chalk Group (green).

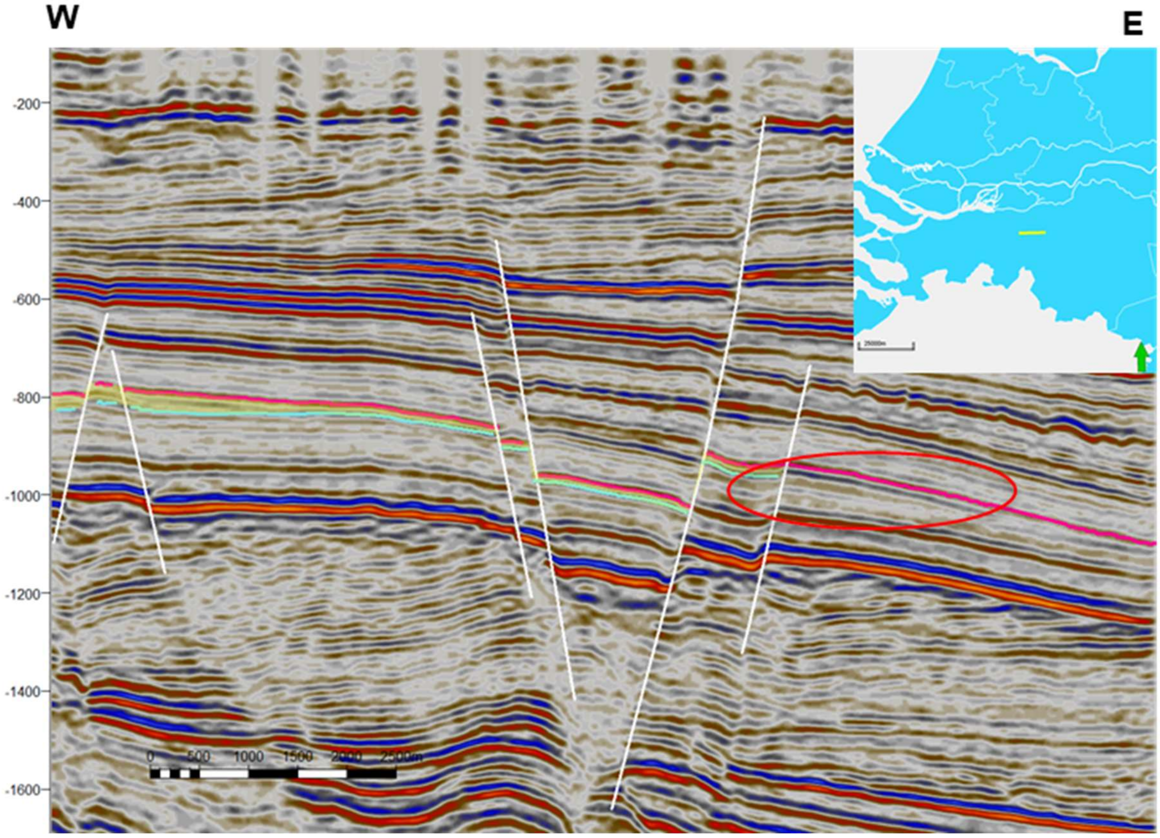

Figure 5-6 Erosion of the BSM by the base Rupel (pink) in the Waalwijk 3D seismic survey. The near base BSM is in light blue. This section demonstrates that the limit of visibility makes it difficult to exactly pinpoint where the BSM disappears. It is probably somewhere in the red ellipse, but it could be further to the west. In the Waalwijk area well penetrations constrain the thickness and distribution of the BSM.

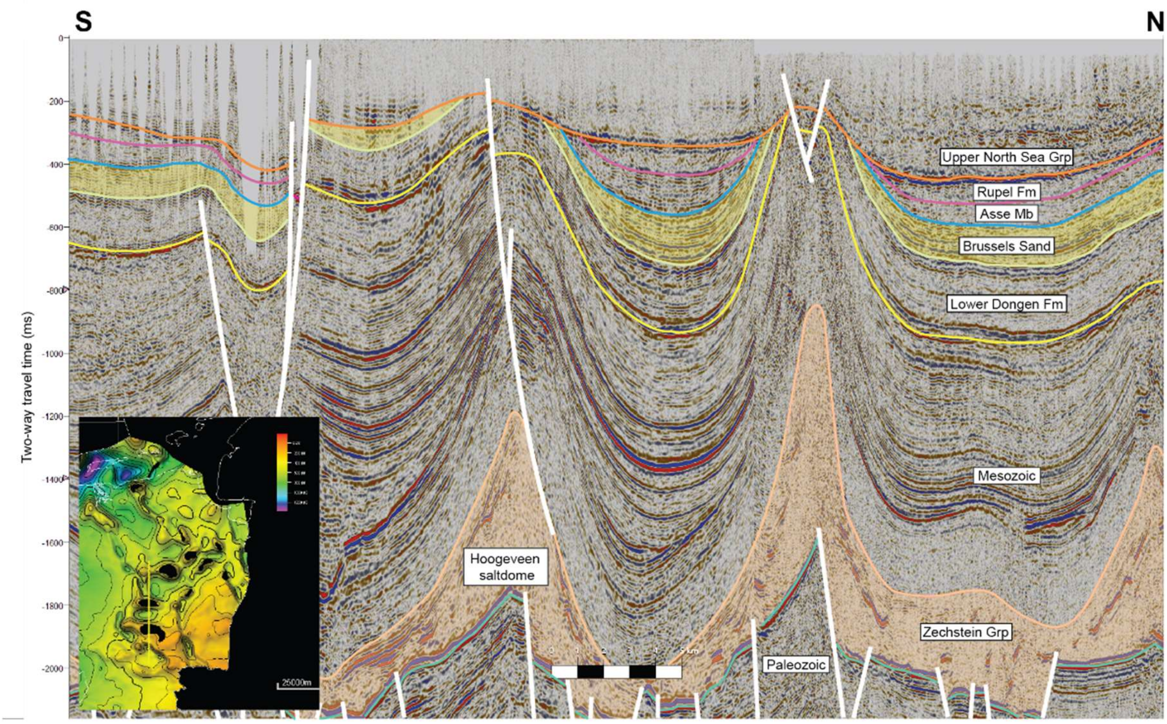

Figure 5-7 BSM occurrence near salt domes in the Province of Drenthe. Note the thickness changes end erosions related to the salt domes.

5.2.3 Uncertainty in seismic interpretation

The observation that there is not always a distinct velocity and/or density break at the top of the BSM implies that the picked top Brussel Sand on seismic data cannot be expected to be exactly at the position of the GR break at the top of the BSM. The unknown phase and polarity of the 2D data results in a picking uncertainty of a quarter of a wavelength (minimum versus zero phase) or even half a wavelength in case the polarity is estimated wrongly. The dominant frequency of the seismic surveys is dependent on acquisition and processing parameters in the range of 30 – 50 Hz corresponding to wavelengths λ of 40 – 70 m. The limit of separability is λ/4 resulting in a range between 10 and 17 m. This means that in principle the top and base of the BSM cannot be mapped separately when the thickness of the BSM is within this range or smaller. Figure 5-6 illustrates that this issue complicates the definition of the pinchout location where the BSM is completely eroded.

Estimation of a wrong polarity results in a mis-pick of half a wavelength (20-35 meter). If the seismic data are minimum phase instead of the assumed zero phase the mis-pick would be a quarter of a wavelength resulting in uncertainty of 10-18 meter. A similar picking uncertainty applies to the base of the BSM as for the top, although one could argue that it could be a bit higher due to a less distinct signature on GR logs. This could mean that the base picked on well logs is prone to mis-interpretation.

Picking data on seismic lines with differing frequency content may result in “jumps” in the interpretation. Figure 5-8 demonstrates that the change in frequency content between crossing lines causes discontinuities in the picking of the top and base of the BSM. This effect is however smaller or in the same order of magnitude as the uncertainty due to polarity and phase.

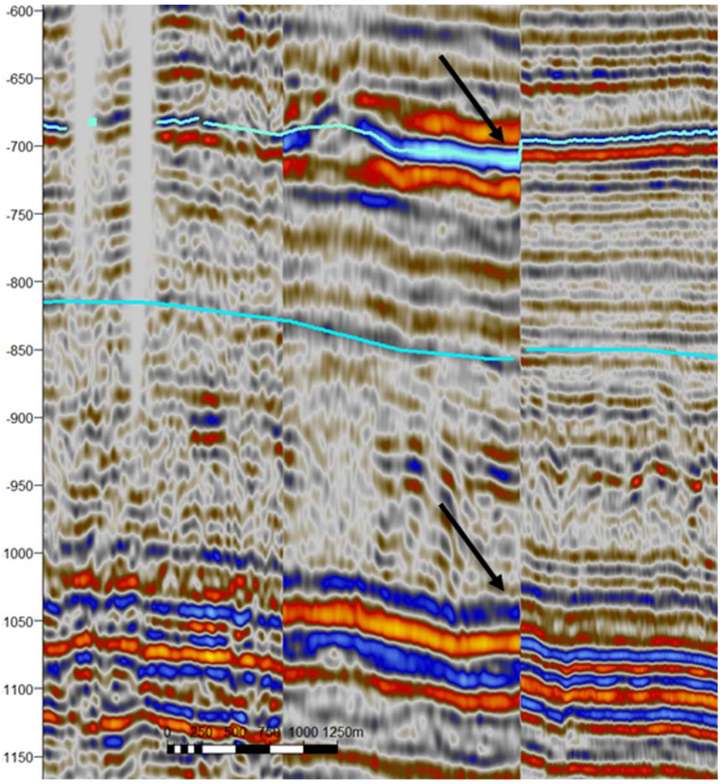

Figure 5-8 The middle part of this seismic section (part of E-W composite section in the South (Appendix 4) has a lower dominant frequency. As a result of this polarity and phase are difficult to align with connecting lines. Tracking minimum and maximum amplitude values will result in jumps in interpretation in the order of 15 ms (15 m at 2000 m/s)

Figure 5-4 shows that changes in frequency content also occur in the SCAN reprocessing of the NAM deep line (L2NAM1982F/L2NAM1984N), which is an amalgamation of various acquisitions. North of this frequency jump the limit of separability is almost twice as high as south of the jump, enabling a far more detailed interpretation.

Finally, the 2D migration of seismic data causes mis-ties between 2D seismic lines. In most cases these mis-ties are not severe due to the relative flat geometry of the BSM. However, local mis-ties in the order of 15-30 ms are observed (Figure 5-9).

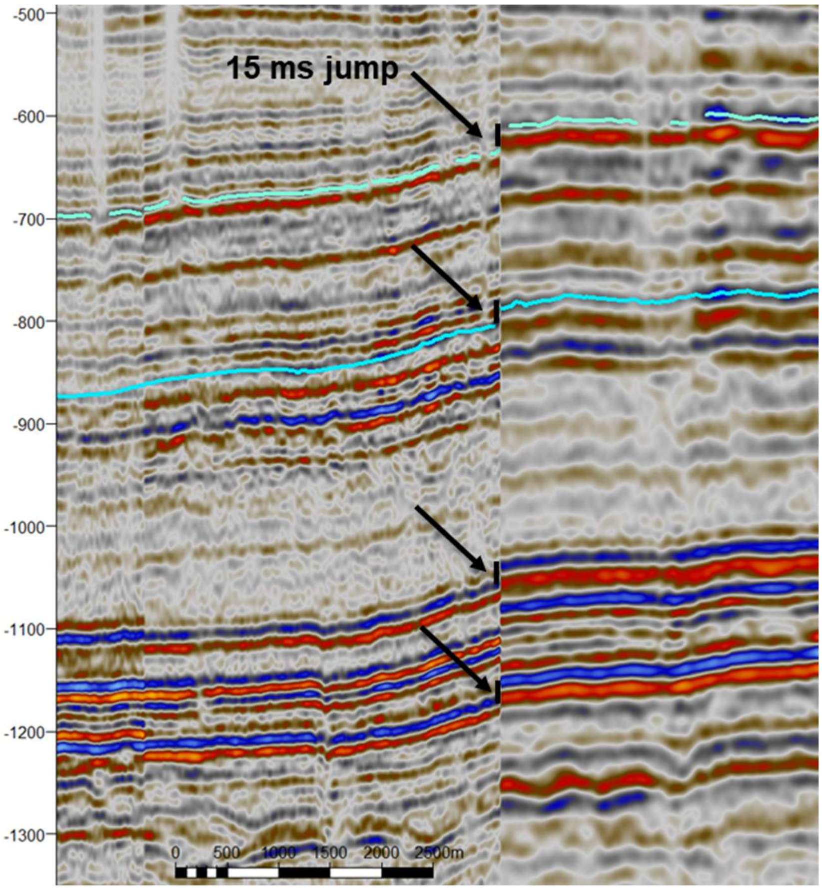

Figure 5-9 Example of a time jump from the W-E composite section in the south (Appendix 4). The time values at the intersection of the two seismic lines show a time difference in the order of 15 ms (15 m at 2000 m/s)

6 Modelling

6.1 Workflow modelling

Figure 6-2 shows an overview of the modelling workflow. Seismic interpretation and well tops are the input for the modelling of the BSM. The seismic interpretation was first converted to datapoints. Next, these datapoints were converted to depth (paragraph 6.2). The modelling, i.e., the generation of top and bottom surfaces, was then performed in the depth domain (true vertical depth or TVD).

Generally, due to erosion, the BSM is partly or even completely eroded in the central parts of the Netherlands. In the former case, the BSM is not overlain by the Asse Member but is covered by the Rupel Formation (Figure 6-1 A). Locally, especially above salt domes, it may be directly covered by the deposits of the Upper North Sea Group (Figure 6-1 B). Therefore, it was necessary to interpret these overlying units locally as well in order to be able to construct a complete top BSM surface. Consequently, the top BSM is a merged surface consisting of the top BSM interpretation and base Rupel/Base Breda interpretation at places where the top of the BSM is eroded. The surfaces where made by using the convergent gridding algorithm.
In the extreme SW (SW Zeeland) where no seismic data is available some shallow wells were used as input to the gridding process. After the gridding a well tie to deep wells was performed by interpolating the well residuals using the moving average algorithm and adding this surface to the top BSM surface.

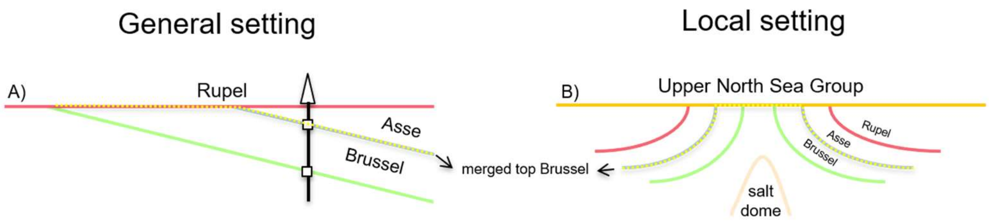

Figure 6-1 Two geological situations for generation of a merged top Brussel surface (yellow dashed line).

The base of the BSM was gridded and subtracted from the constructed top BSM surface to arrive at a thickness grid of the BSM, based on seismic interpretation data only. In the gridding process the polygon with thickness value zero, delineating the location of the pinch-out of the BSM, was used as input to the gridding process. A residual thickness map was then produced by calculating the residual thickness at the well locations and interpolating these values. The pinch-out polygon was used to guide the interpolation to ensure a zero thickness at the location of the polygon. In this way a tie to the wells was ensured (see paragraph 6.4). This tied thickness map was added to the tied top BSM map to arrive at a tied base BSM, being base S2 in the North and base S1 in the South. A well-based thickness map of the S1 cycle was made that was used to construct the base S1 and base S2 surfaces in the northern and southern areas, respectively. This approach allows to either include or exclude the S1 cycle from the Brussel Sand for reservoir modelling purposes the involve its flow properties.

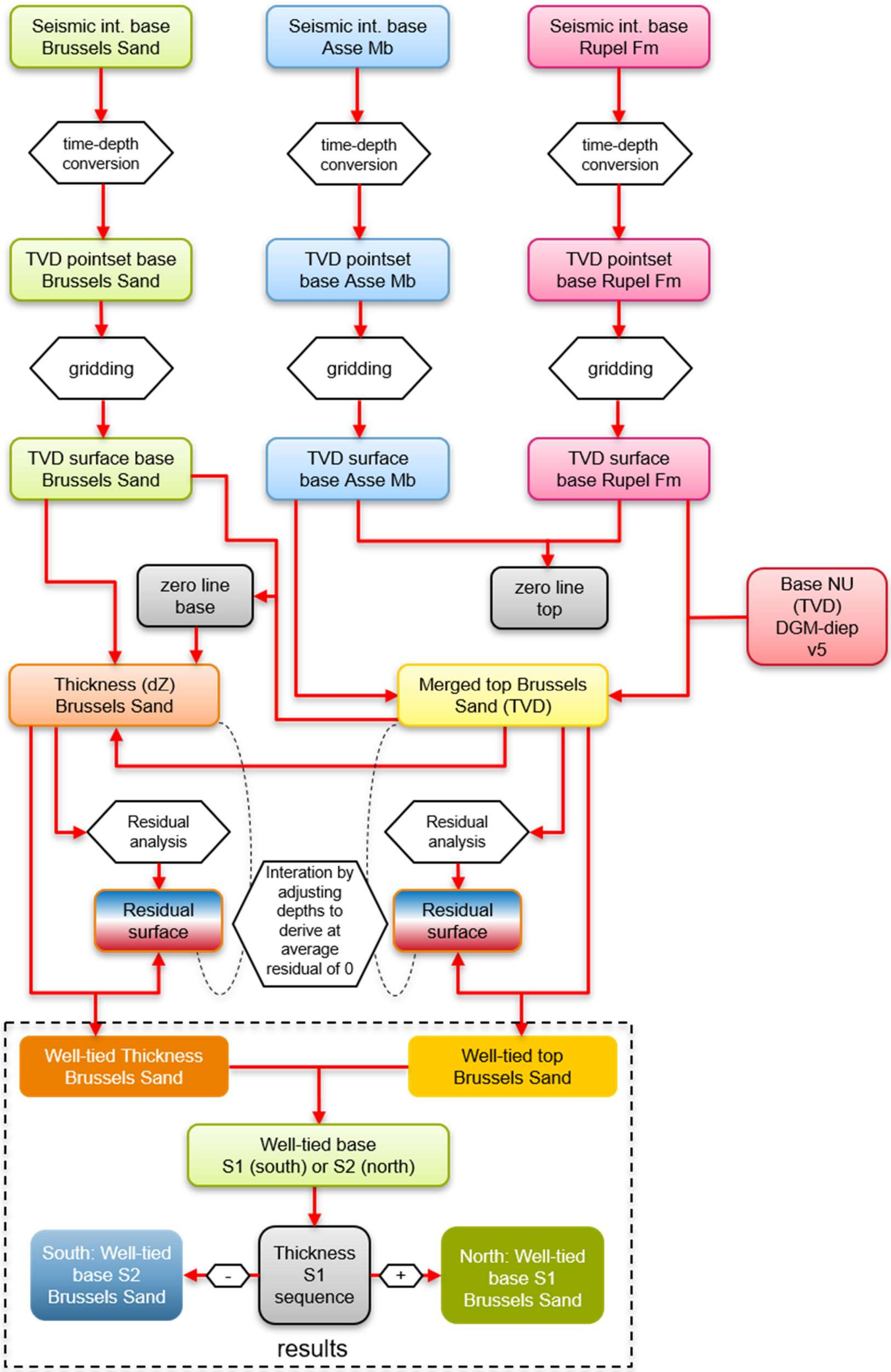

Figure 6-2 Applied modelling workflow.

6.2 Time-Depth Conversion

The limited availability of sonic log data in the Paleogene interval challenges the construction of a velocity model for this interval. However, the Velmod 3.1 model (Pluymaekers et al. 2017) makes use of a large number of wells with sonic and/or check-shot data. Figure 6-3 combines the interval velocities of the BSM and the velocity trend for the North Sea Group as defined in the Velmod model. It shows that the observed BSM interval velocities in wells are in line with the model, albeit on average slightly higher. Using the constant k (0.284 s^{-1}) and V0 (1788 m/s) value as derived in the Velmod study in the time depth conversion process results in an unbiased prediction of the Depth of the top of the BSM (see well residuals in paragraph 6.4).

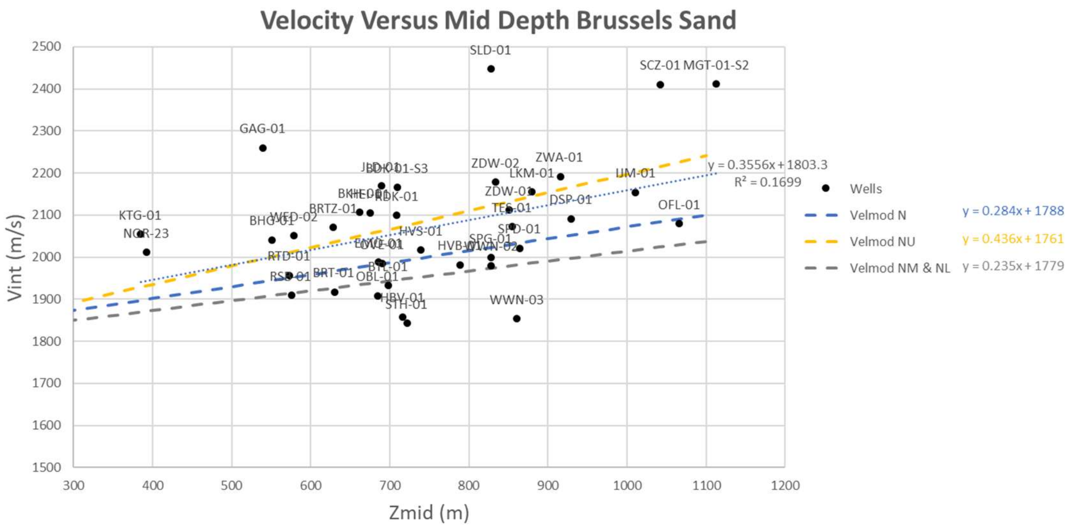

Figure 6-3 Interval velocity (Vint) of the BSM plotted against Mid-depth (Zmid). The interval velocity of the wells is on average slightly higher than the velocity functions from the Velmod model predict for the Lower and Middle North Sea Group. However North Sea Group velocity function gives an unbiased prediction for the top BSM as witnessed by the residuals.

The uncertainty associated to the time-depth conversion of Top BSM is indicated by the standard deviation (SD) of the Vint and V0 maps in the Velmod report. In areas that are remote from well control the SD is in the order of 100 m/s, being in the order of 5% of the average interval velocity. Assuming a normal distribution of the error, this means that 68% of the wells will be predicted within a depth range of 50 m (SD) and 95% within a depth range of 100 m (2 SD) if the top BSM lies at 1000 m. These numbers are maximum numbers since most areas are closer to well control. By applying a constant V0 instead of a gridded V0 the depth residuals at wells can serve as an indication of uncertainty. Paragraph 6.4 demonstrates that the standard deviation of the well residuals at top BSM is in the order of 20 m, which is substantially less than the 50 meters calculated above.

6.3 Top, base and thickness of BSM maps

Maps of the top and base of the BSM can be found in Appendix 3. The top and base BSM maps show the greatest depth along a NNW-ESE trending zone from Vlieland to Amersfoort-Apeldoorn (known as the "Zuiderzee low") and in the Roer Valley Graben in Brabant. In eastern Drenthe and Overijssel and in Zeeland the BSM is buried shallowly, or even eroded. In a central strip running from Alkmaar-the Hague in the WNW to Arnhem-Eindhoven in the ESE the BSM is eroded by the base Rupel Formation or base Breda Formation. The thickness map of the Brussel Sand clearly shows that the thickness of the BSM decreases towards this zone, which is considered to have been a high during deposition of the Brussels. The absence of the BSM top suggests that is was affected by later local erosion as well. The thickest occurrence of the BSM can be found just SW of this high in a WNW-ESE trending zone just south of Rotterdam (known as the “Voorne Trough”), where it reaches a thickness up to 200 meters. Also, in the North of Overijssel, South Friesland and in the northern part of the IJsselmeer up till Texel and Vlieland the thickness of the BSM exceeds 100 meters.

6.4 Tying to wells and residuals

The tying of the maps to the wells has been limited to wells with good quality well log data in which both the top and base of the BSM could be picked with confidence. Appendix 1 contains the depth residuals for the top Brussels, and Figure 6-4 shows the residual map. The average mis-tie is three meters with a standard deviation of 20 meters.
The tying of the thickness map resulted in a residual map (Figure 6-5) and residuals tabulated in Appendix 4 The average mis-tie of the thickness of the BSM is 10 meters with a standard deviation of 30 meters. There is a small bias towards a thicker BSM on seismic than in wells. The main cause for the rather large standard deviation is caused by the uncertainty in picking the base of the BSM on seismic and in wells. The standard deviation for the picking base BSM is also 30 meters.

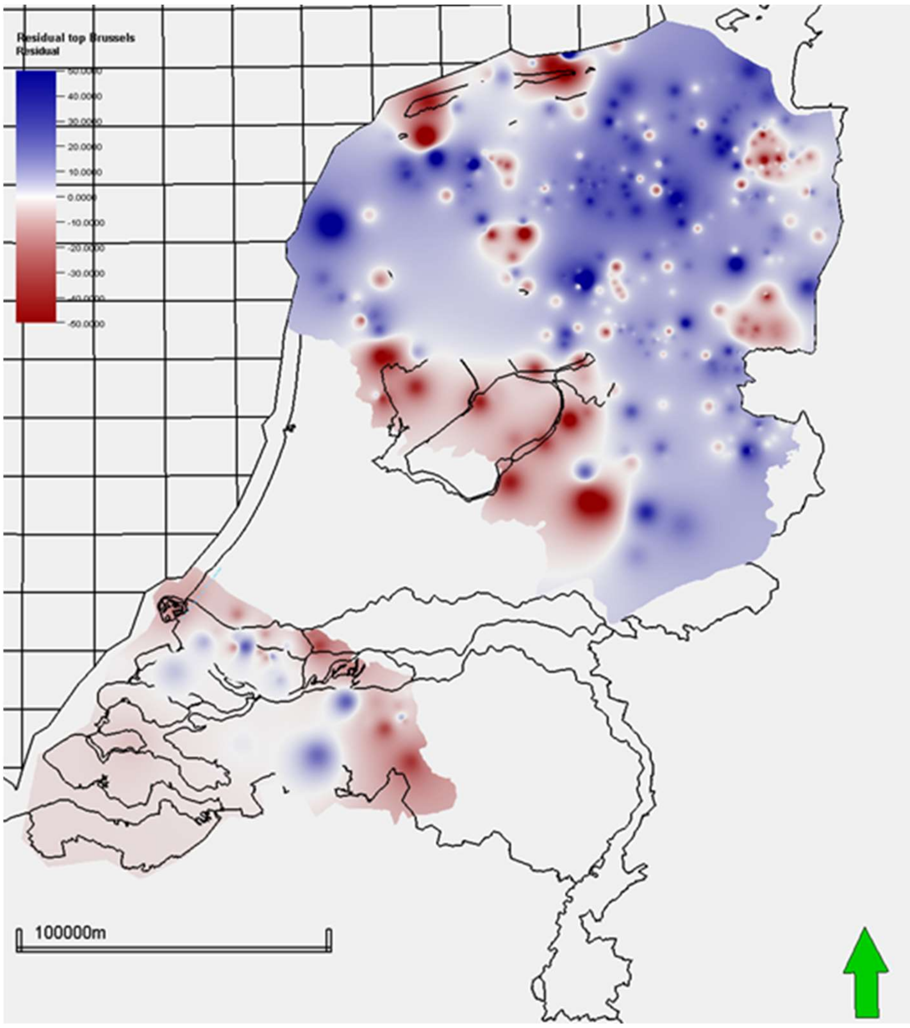

Figure 6-4 Residual (m) between top BSM in the well and in the Gridded top BSM surface before well tie. Positive numbers (blue) indicate that the surface is deeper than the well top.

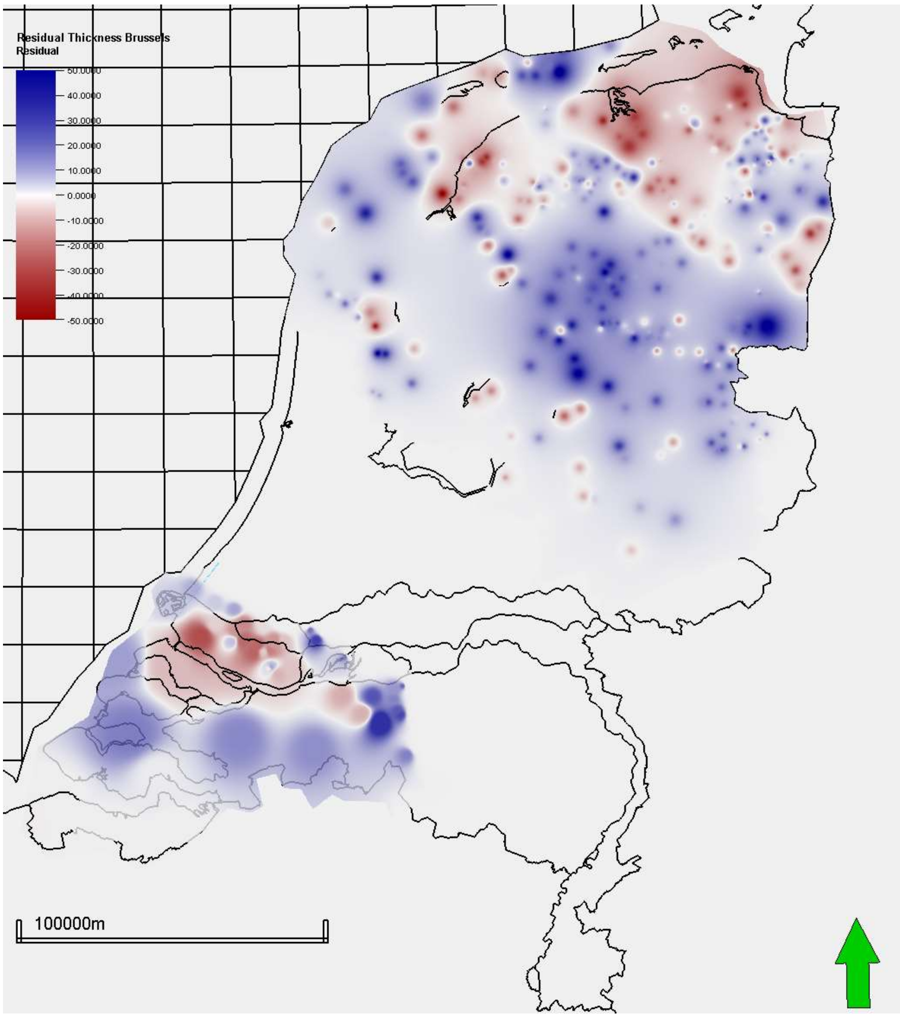

Figure 6-5 Residual (m) between thickness of the BSM in the well and in the thickness grid before well tie. Positive numbers (blue) indicate that the surface is thinner in the grid than in the well.

7 Discussion and Conclusions

The aim of this project was to update the regional top depth and thickness maps of the BSM with the aim of enabling an improved geothermal potential estimate in ThermoGIS.

A comparison with the previous (well-based) maps of the BSM learns that improvements are mainly seen in the thickness map and the depth map of the base of the BSM. Both show on the one hand a smoother thickness distribution than the earlier maps that suffered from inconsistencies in well picks that lead to bull's-eyes, and on the other hand an increased spatial resolution caused by the abundant use of seismic data. The previous inconsistent interpretation of the base of the BSM, either at base S1 or base S2, was the main cause of the bull's-eyes. Another important improvement is the improved definition of the boundary polygon enclosing the distribution of the BSM. There is no noticeable change in the average depth of the Brussel Sand. An overall increase of the average thickness is attributed to the consistent incorporation of the S1 sequence sands. This especially holds for the northern area where the base of the BSM used to be placed at the base of the S2 sands.

In order to generate this set of maps, a vast set of wells and seismic data were evaluated in a relatively short time span. This means that the maps are not suitable for local geothermal prospect evaluation. For these kinds of studies a more detailed mapping incorporating all wells and seismic lines in the vicinity would be required. Quantitative interpretation, like extracting properties form intervals within the BSM could shed a light on the local development of the BSM in areas where 3D seismic data is available. New acquisition or processing of seismic data, such as currently carried out in the SCAN project framework, might be recommendable for such studies.

An attempt was made to map the limit of the BSM distribution by using seismic data. The limited resolution of the seismic data however prevents to distinguish the sand where the thickness is below approximately 15 meters. This means that there is a zone around the outer limit of occurrence in which it is unsure if the BSM is present and, if present, what the thickness is.

The thickness variation of the BSM is mainly determined by the erosion of its top at structural highs or at flanks of salt domes. However, it is also observed that the unit thins towards the highs and salt domes in the area unaffected by erosion. This indicates that during the deposition of the BSM the highs became (slightly) uplifted and in this same period active halokinesis (salt doming) took place.

The total uncertainty in depth and thickness of the BSM is caused by several inaccuracies:

1. The polarity and phase of the seismic data is not always known. Therefore it is uncertain which event should be picked (peak, trough, zero crossing or different). in the absence of sufficient knowledge about the right polarity and misjudging an improperly chosen event could lead to an error of 20-35 meters, depending on the frequency.
2. The seismic resolution is especially an issue in areas where the BSM is thin and pinching out.
3. The top and base BSM as defined on the GR log does not always coincide with a (clear) break on the sonic and/or density log. The acoustic response of the top and base are mostly an interference pattern of impedance contrasts within a wavelength distance from the event.
4. Seismic frequency content and hence seismic resolution causes interference pattern differences between seismic surveys.

5. Vertical mismatches up to 15-30 ms TWT (15-30 meters at 2000 m/s) are observed at intersections of crossing 2D seismic lines. These are caused by imperfect migration (of 2D seismic lines) in combination with uncertainty in statics (topography and reference to seismic datum).
6. P-wave velocities in the overburden and in the BSMvary laterally. The process of velocity model building and time-depth conversion has an uncertainty illustrated by the scatter of well interval velocities around the used velocity function. The uncertainty in velocity could lead to 5% uncertainty in depth. This translates into 50 meters uncertainty at a depth of 1000 meters.
7. The total uncertainty depends on data density. Close to wells and seismic lines the uncertainty is smaller than in areas remote from data.
8. An indication of the total uncertainty is provided by the well residuals. The well residuals show a standard deviation of 20 meters for the top and 30 meters for the base of the BSM. This means (assuming a normal distribution) a probability of 68% that the predicted depth will be within 1 standard deviation, and 95% that it will be within 2 standard deviations (being ± 40 meters for the top and ± 60 meters for the base of the Brussel Sand). In areas remote from well and seismic data the uncertainty will be larger.

8 References

Collinson, M.E. & Cleal, C.J., 2001a. The palaeobotany of the Palaeocene and Palaeocene-Eocene transitional strata in Great Britain. In Cleal, C.J., Thomas, B.A., Batten, D.J., Collinson, M.E. (eds), Mesozoic and Tertiary palaeobotany of Great Britain. Geological Conservation review Series No. 22, Joint Nature Conservation Committee, Peterborough, 155-184.

Collinson, M.E. & Cleal, C.J., 2001b. Late Middle Eocene-early Oligocene (Bartonian-Rupelian) and Miocene palaeobotany of Great Britain. In Cleal, C.J., Thomas, B.A., Batten, D.J., Collinson, M.E. (eds), Mesozoic and Tertiary palaeobotany of Great Britain. Geological Conservation review Series No. 22, Joint Nature Conservation Committee, Peterborough, 227-274.

Gibbard, P. L., & Lewin, J. (2016). Filling the North Sea Basin: Cenozoic sediment sources and river styles (André Dumont medallist lecture 2014). *Geologica Belgica* 19/3-4: 201-217.

Knox, R.W.O'B., Bosch, J.H.A., Rasmussen, E.S., Heilmann-Clausen, C., Hiss, M., De Lugt, I.R., Kasińksi, J., King, C., Köthe, A., Słodkowska, B., Standke, G. & Vandenberghe, N., 2010. Cenozoic. In Doornenbal, J.C. & Stevenson, A.G. (eds), Petroleum geological atlas of the Southern Permian Basin area. EAGE Publications b.v., Houten, 211-223.

Munsterman, D.K., 1999. De resultaten van het dinoflagellatenonderzoek naar de ouderdom en het afzettingsmilieu van boring DON-01 (Dongen-01), traject: 532*1016.5 m. TNO Rapport NITG99-194-B.

Munsterman, D.K., 2002. De resultaten van het dinoflagellatenonderzoek naar de kernen van BPM boring Raalte-1. TNO rapport NITG02-046-B.

Munsterman, D.K., 2017. De resultaten van het palynologische onderzoek naar geselecteerde zandige intervallen van boringen SPG-01, WWN-01, WWK-01 and GWD-01. TNO Rapport R10669.

Munsterman, D.K., 2018 De resultaten van het palynologische onderzoek naar het Paleogeen en Neogeen van boring Rijsbergen-01 (RSB-01), interval 50-900 m. Rapport TNO 2019 R11086 (DGM-Diep>H3O De Voorkempen).

Munsterman, D.K., 2020a. De resultaten van het palynologische onderzoek naar de ouderdom van boring Oudega-Akkrum (AKM-03), interval 204-1098 m. TNO Rapport 10477.

Munsterman, D.K., 2020b. De resultaten van het palynologische onderzoek naar de ouderdom van boring Zuidwal-02 (ZDW-02): 310-1280 m. TNO Rapport R11010.

Munsterman, D.K. and Kerstholt-Boegehold, 2015. De resultaten van het palynologisch onderzoek naar de ouderdom van boring Hilvarenbeek-01 (HVB-01), interval 780-1000m. TNO Rapport R10700.

Pluymaekers, M.P.D., Doornenbal J.C. and Middelburg H. (2017)– *Velmod 3.1 TNO report*

Schroot B.M. and de Haan, H (2003) – An improved regional structural model of the Upper Carboniferous of the Cleaver Bank High based on 3D seismic interpretation. Geological Society of London, Special Publication 212, page 23-37

Sluijs, A., Brinkhuis, H., Crouch, E. M., John, C. M., Handley, L., Munsterman, D. & Pancost, R. D. (2008). Eustatic variations during the Paleocene‐Eocene greenhouse world. *Paleoceanography*, *23*(4).

Vrijlandt, M.A.W., E.L.M. Struijk, L.G. Brunner, J.G. Veldkamp, N. Witmans, D. Maljers, J.D. van Wees. 2019. ThermoGIS update: a renewed view on geothermal potential in the Netherlands. EGC, The Hague, June 2019.

9 Appendices

Appendix 1 Residuals

Well	Top	Base	Thickness
AHO-E-S5	-4.66	51.21	55.87
AKM-01	-5.79	24.96	30.75
AKM-02	-6.71	5.56	12.35
AKM-03	-10.67	47.2	57.86
AKM-04	-0.97	11.51	12.47
AKM-05	-44.52	28.35	72.85
AKM-17	11.9	17.66	5.7
ALD-01	-21.15	0.46	21.61
AME-103	-65.23	-90.42	-25.23
AME-103-S	-65.23	-90.42	-25.23
AME-202	-18.64	-55.81	-37.26
AME-202-S	-18.57	-55.27	-36.78
AME-205	-15.42	-49.31	-33.95
AME-205-S	-15.42	-49.31	-33.95
AME-205-S	-15.42	-49.31	-33.95
AML-01	-24.33	-12.01	12.36
AMN-01	-23.71	127.75	151.46
AMO-01	-23.39	20.6	44
AMO-02	-23.22	0.28	23.65
AMO-03	-16.42	3.29	19.78
AMO-04	3.09	58.54	55.45
AMR-01	-24.48	-1.88	22.6
ANA-01	3.83	19.11	15.28
ANJ-01	12.57	41.33	28.59
ANN-01	-9.76	4.35	14.11
ANS-01	-10.25	0.79	11.04
ANV-03	-33.77	-3.57	29.79
APN-01	-3.03	-59.59	-56.56
APN-02	8.94	-92.72	-101.67
APS-01	-15.87	15.48	31.39
ASN-01	-4.19	-11.11	-6.92
Average	**-15.50**	**-4.59**	**10.89**
BAR-NE-0	15.05	-3.06	-18.14
BAS-03	-20.58	134.73	155.21
BAS-04	39.39	-14.88	-54.27
BDK-01	1.84	-0.92	-2.74
BDK-01-S1	1.84	-0.92	-2.74
BDK-01-S2	1.84	-0.92	-2.74
BDK-01-S3	1.84	-0.92	-2.74
BDM-01	-9.25	7.38	16.63
BDM-02	-11.52	-24.01	-12.49
BHG-01	-1.62	12.88	14.5
BHH-01	-18.92	4.89	23.76
BHM-01	-10.45	15.73	26.19
BHM-06	-18.51	-14.78	3.9
BIR-01	5.84	16.12	10.26
BIR-02	21.34	36.01	14.68
BIR-02-S1	17.8	31.3	13.5
BIR-03	15.34	26.65	11.32
BIR-13	17.93	28.35	10.41
BKH-01	5.8	11.87	6.05
BKZ-01	0.41		
BLF-101	3.9	20.69	16.8
BLF-108	-10.05	9.85	19.87
BLH-01	-21.73	7	28.72
BLK-01	10.71	-11.62	-22.33
BLS-01	-23.84	-2.34	21.53
BLS-01-S1	-23.84	-2.34	21.53
BLS-02	-27.05	-4.05	22.54
BNT-01	-28.48	-17.04	11.44
BOL-01	10.75	-1.03	-11.78
BOZ-01	10.44	8.7	-1.74
BRA-01	-10.11	-6.7	3.33
BRG-01	5.41	91.62	86.24
BRH-01	24.86	34.65	9.95
BRL-01-S1	-40.83	-9.31	31.53
BRT-01	-2.21	-20.13	-17.92
BRTZ-01	3.48	-5.78	-9.26
BRW-01	14.06	11.36	-2.67
BRW-01-S	14.06	11.36	-2.67
BRW-01-S	14.06	11.36	-2.67
BRW-02	12	9.78	-2.19
BRW-04	12.09	8.98	-3.07
BTA-01	-7.94	-1.35	6.7
BTL-01	4.33	-12.6	-16.93
BUI-01	-12.19	18.03	30.22
BUR-01	-33.25	-15.16	18.21
BWD-01	-34.64	36.53	71.18
CLDV-01	-26.18	20.71	46.58
CLDV-01-S	-26.18	20.71	46.58
COC-01	-18.93	10.68	29.61
COV-03	-6.73	15.86	22.51
COV-05	-23.87	36.41	60.29
DAL-01	-40.76	-31.06	9.85
DAL-02	-16.65	-19.01	-2.19
DAL-02-S1	-16.65	-19.01	-2.19
DHV-01	-51.54	-2.98	48.78
DIV-01	-9.29	2.15	11.44
DJM-01	34.44	8.92	-25.52
DJM-01-S1	34.44	8.92	-25.52
DKK-01	-0.84	38.09	38.93
DKK-02	-0.84	38.09	38.93
DON-01	-0.01	6.67	6.68
DRM-01	-4.99	15.25	20.28
DRM-01-S	-4.99	15.25	20.28
DRP-01	-3.83	-30	-26.19
DSP-01	-11.55	-37.31	-25.76
DSP-02	22.34	-72.71	-94.87
DVD-02	-24.88	20.81	45.7
DVN-01	-2.37	5.09	7.42
DWL-01	-10.05	0.99	11.04
DWL-02	-23.47	6.9	30.37
DZL-01	-5.47	20.78	26.17
DZL-OBS	-5.84	18.35	24.08
EKL-01	15.33	44.12	28.54
EKL-12	17.66	48.75	30.92
EKL-13	20.76	47.74	26.95
EKR-104	-1.67	6.75	8.52
EKR-104-S	-1.67	6.75	8.52
EKR-208	-1.52	-0.21	1.3
ELV-101	20.36	11.04	-9.14
EMM-04	27.6	10.36	-17.33
EMO-01	-19.04	7.9	26.94
ENA-01	-62.26	-16.61	45.64
ENA-01-S2	-62.26	-16.61	45.64
ENA-02	-64.2	-16.72	47.48
ENA-02-S1	-64.2	-16.72	47.48
EPE-01	9.43	21.43	12.01
ERM-01-S1	12.02	-43.76	-55.69
ERW-01	4.78	3.07	-1.71
ESG-01	-19.2	-15.06	4.15
ESV-01	-32.45	-9.38	23.05
ETV-01	-20.28	13.2	33.45
ETV-01-S1	-20.28	13.2	33.45
ETV-01-S2	-20.28	13.2	33.45
EWM-01	41.38	52.33	10.95
EXO-01	1.83	1.61	0.49
EXO-02	-0.8	1.04	1.84
EXO-02-S2	-0.8	1.04	1.84
EXO-02-S4	-0.8	1.04	1.84
FRB-01	-25.29	-26.42	-1.2
GAG-01	-2.3	-0.02	2.28
GGT-102	32.47	31.84	-0.63
GGT-102-S	32.47	31.84	-0.63
GGT-102-S	32.47	31.84	-0.63
GGT-102-S	32.47	31.84	-0.63
GGT-103	42.24	31.2	-11.04
GIT-01	-22.36	-0.75	21.58
GLH-01	-2.19	-17.1	-15.02
GRK-01	32.45	-14.53	-46.95
GRK-01-S1	32.45	-14.53	-46.95
GRL-01	4.72	-0.95	-6.18
GRW-01	6.08	19.82	13.68
GST-01	-7.13	5.73	12.86
GSV-01	7.39	16.29	8.9
GSV-01-S1	7.39	16.29	8.9
GSV-01-S2	7.39	16.29	8.9
HBG-02	-5	22.34	27.34
HBG-02-S1	-5	22.34	27.34
HBG-03	-2.32	17.69	20.01
HBV-01	-15.91	33.13	49.04
HEI-01	-3.49	-22.16	-18.67
HES-01	-23.76	-1.8	21.92
HGM-01	17.89	-4.3	-22.2
HGZ-01	-2.86	-36.97	-34.11
HIJ-01	-17.04	18.28	35.43
HLD-01	10.72	7.02	-3.59
HLE-01	1.7	6.32	4.61
HNS-01	-6.76	-11.21	-4.45
HOA-01	13.25	11.62	-1.65
HOA-01-S	13.25	11.62	-1.65
HOA-03	10.51	-5.78	-16.3
HOK-02	8.94	8.76	-0.18
HRL-01	7.28	13.01	5.72
HRL-02	1.45	3.34	1.92
HRL-03	17.18	13.53	-3.55
HRL-10	13.06	6.69	-6.3
HRL-101	14.87	26.61	11.79
HRL-10-S1	13.06	6.69	-6.3
HRL-10-S2	13.06	6.69	-6.3
HRL-10-S3	13.06	6.69	-6.3
HRS-01	-1.7	48.94	50.64
HRS-01-S1	-1.7	48.94	50.64
HRV-01	-21.42	16.6	38.02
HTM-01	14.63	-8.88	-23.52
HTM-01-S	14.63	-8.88	-23.52
HVB-01	-28.87	-12.71	16.16
HVS-01	6.76	-31.03	-37.79
IJD-01	16.12	-22.56	-38.68
IJM-01	-18.63	-39.81	-21.18
IJP-01	16.39	4.87	-11.59
JLD-01	-4.18	20.43	24.61
JPE-01	-7.33	38.66	45.99
KAM-01	-55.16	-9.32	45.79
KAM-01-S	-55.16	-9.32	45.79
KGB-01	-47.24	-36.93	10.32
KHM-01	-4.42	47.34	51.72
KMP-01	16.05	12.6	-3.71
KMP-02	9.18	5.54	-4.16
KOL-02	26.04	29.54	3.49
KOM-01	-12.15	-9.75	2.25
KRL-01	-17.73	5.52	23.29
KTG-01	0.59	15.82	15.23
LEL-01	12.87	-42.85	-55.72
LEW-01	-10.34	34.62	45.1
LKM-01	-56.8	-68.12	-11.32
LMB-01	43.08	24.48	-18.63
LNH-01	-43.99	-5.83	38.16
LOM-01	-15.29	16.45	31.74
LOM-02	-6.79	18.75	25.55
LOZ-01	-0.87	34.46	35.33
LRM-01	36.7	16.43	-19.97
LTG-01	-30.46	-15.61	14.85
LWO-01	15.71	32.67	16.97
LWO-01-S	15.71	32.67	16.97
LWO-01-S	15.71	32.67	16.97
LWZ-02	28.1	8.98	-19.11
LWZ-03-S1	23.01	20.4	-2.61
MAL-01	-35.22	-10.81	24.55
MAR-101	10.24	39.11	28.87
MBN-02	-10.63	27.48	38.13
MDM-01	11.22	11.01	-0.47
MDM-02	16.9	22.08	6.09
MDM-02-S	16.9	22.08	6.09
MDM-02-S	16.9	22.08	6.09
MDN-01	-1.8	-12	-10.2
MEE-01	19.04	-130.28	-149.32
MID-101	-7.39	3.21	10.59
MID-201	-8.52	-36.24	-27.72
MKN-01	-45.45	26.34	71.79
MKO-01	8	31.38	23.42
MKO-01-S	8	31.38	23.42
MKZ-01	35.27	-2.82	-38.09
MKZ-01-S1	35.27	-2.82	-38.09
MKZ-06	29.36	4.3	-25.09
MSV-01	-18.71	-13.24	5.47
MWD-02	-7.45	-11.09	-4.02
NAG-01	-23.54	-37.33	-13.79
NBG-01	-11.22	-4.38	6.74
NDP-01	-10.89	-22.73	-11.84
NGA-01	-0.95	18.51	19.34
NGA-02	6.15	32.9	26.69
NGA-02-S	6.15	32.9	26.69
NGA-02-S	6.15	32.9	26.69
NGA-04	-16.95	24.41	41.34
NGA-07	-14.23	19.47	33.75
NLM-01	-17.2	20.33	37.64
NMD-01	2.48	12.91	10.43
NMD-02	1.86	0.86	-1
NNE-01	14.88	-5.9	-20.78
NNE-03	8.43	-12.2	-20.63
NNE-06	-11.13	-18.52	-7.39
NNE-07	4.81	-33.03	-37.76
NNE-09	22.79	4.27	-18.09
NOR-01	-5.38	23.46	28.43
NOR-03	14.65	20.13	5.42
NOR-21	14.52	61.01	46.49
NOR-23	1.32	64.51	63.19
NOR-31	8.94	61.87	52.94
NOR-33	5.87	55.03	49.16
NOR-35	6.98	68.05	61.08
NRD-01	19.62	44.08	24.46
NRZ-01	26.9	48	21.84
NSL-01	-33.25	-13.63	19.66
NSN-01	6.8	7.54	0.75
NWH-01	-25.13	25.73	50.86
NWS-01	6.24	-12.38	-18.85
OAS-01	-32.88	-0.7	32.18
OBL-01	-10.55	-41.27	-30.72
OBLZ-01	0.11	-30.34	-30.45
ODS-01	-8.84	14.24	23.1
OFL-01	4.88	-18.35	-23.21
OLD-01	6.01	3.78	-2.15
OLR-01	-17.23	39.93	57.14
OLR-02	-22.72	12.73	35.69
OMM-02	-24.71	3.1	27.82
OMM-03	-11.74	-10.75	0.85
OPE-01	-10.79	18.8	29.61
OPE-02	-7.86	29.32	37.21
OPH-01	-1.89	-96.83	-94.94
OPO-01	-13.4	32.51	45.91
OVE-01	4.51	-13.06	-17.57
OVS-01	13.37	18.74	5.56
OWD-01	-16.59	24.95	40.97
OWG-01	-8.71	-14.61	-6.11
PAU-01	5.87	13.8	7.93
PBR-01	14.97	18.68	3.71
PEI-01	7.94	-19.49	-27.4
PRW-01	2.26	-21.45	-23.71
PSP-01	-5.18	31.99	37.16
PSP-03	17.04	20.55	3.51
RAL-01	-3.21	19.92	23.25
RDK-01	-10.25	-18.43	-8.18
REU-01	-18.46	0.79	19.28
ROD-102	26.24	28.25	2
ROT-01	-30.86	-54.37	-23.51
ROT-01-S1	-30.86	-54.37	-23.51
RPL-01	-38.89	-4.5	34.39
RSB-01	19.02	32.52	13.5
RSW-01	11.09	35.78	24.62
RSW-02	5.93	37.74	31.75
RTD-01	-11.49	-16.4	-4.91
RUI-01	13.52	60.29	46.76
RVW-01	-12.39	9.76	22.15
RZB-01	-2.88	-10.27	-7.39
SAN-01	1.05	3.81	2.76
SAP-11	23.69	4.9	-18.79
SAU-01	24.81	37.11	12.3
SCB-01	10.66	0.48	-10.45
SCZ-01	-12.46	-10.56	2.31
SDB-01	-12.33	-51.71	-39.35
SDM-01	9.78	25.31	15.52
SGZ-01	-10.63	-0.58	10.05
SHV-01	-14.54	5.79	20.33
SIB-01	-13.79	17.4	31.19
SLB-01	-32.18	-3.01	29.25
SLB-02	-32.41	-6.9	25.47
SLD-01	3.15	-0.42	-3.59
SLD-02	2.51	10.56	8.05
SLD-03	-5.25	6.16	11.36
SLD-04	2.96	3.13	0.15
SLK-01	-11.67	81.45	93.14
SLN-02	-12.7	-49.47	-36.77
SLN-03	0.92	-0.1	-1.03
SML-01	8.61	11.89	3.39
SMR-01	12.78	7.49	-5.33
SND-01	-43.1	-16.58	26.57
SNK-01	12.4	4.51	-7.74
SNK-02	20.07	17.7	-2.37
SOL-02	16.98	100.8	83.83
SOW-01	-3.22	308.62	311.85
SPG-01	-8.71	9.86	18.57
SPH-01	13.48	-6.74	-19.65
SPI-101	0.95	4.99	4.04
SPKO-01	23.59	-7.75	-31.34
SPKO-02	22.91	-11.54	-34.45
SPKW-01	-14.68	-7.18	7.5
SSM-04	0.87	21.77	20.77
STA-03	-8.87	14.45	23.32
STB-01	-0.69	15.46	16.15
StDev	**18.98**	**39.79**	**38.94**
STE-01	-29.74	-1.37	28.08
STH-01	20.36	8.55	-11.81
STK-01	-19.98	-4.91	14.67
STK-01-S1	-19.98	-4.91	14.67
STK-01-S3	-19.98	-4.91	14.67
STN-01	10.33	14.39	4.77
STN-02	24.32	-7.22	-31.54
STR-01	-0.46	-7.99	-7.53
STW-01	4.78	-4.53	-9.31
SUW-01	14.01	14.75	0.73
SUW-01-S	13.76	15.32	1.56
SWD-01	-21.62	3.73	25.35
SWO-01	-11.57	-18.77	-7.2
SZW-101	12.51	-3.4	-15.25
TBR-04	12.76	51.5	38.74
TER-01	-15.06	-44.62	-29.56
TER-01-S1	-15.06	-44.62	-29.56
TER-01-S2	-15.06	-44.62	-29.56
TES-01	19.94	11.53	-8.42
TID-101	-16.58	17.99	34.57
TID-103	-16.86	19.07	35.94
TID-201	-0.2	30.12	30.44
TID-202	-13.34	19.48	33.27
TID-203	-6.66	23.6	30.59
TID-301	-20.02	24.52	44.54
TID-702	-21.37	21.36	42.73
TJM-01	-11.88	-9.49	2.43
TUB-02	5.43	-0.55	-5.98
TUB-08	-1.04	-2.05	-1.03
TUM-01	-13.68	4.41	18.09
TUM-02	-2.5	23.01	25.41
TUS-01	-10.64	-27.27	-16.49
UHM-01	17.63	36.79	19.16
UHM-01-S	17.63	36.79	19.16
UHM-02	19.74	40.26	20.51
UHZ-01	11.25	14.57	3.32
URE-01	4.42	38.73	34.32
USQ-01	9.51	11.38	1.87
UTB-01	-11.8	-7.06	4.47
UTB-01-S1	-11.8	-7.06	4.47
VKG-01	-14.78	-9.78	5
VLN-01	-14.45	-5.82	8.63
VLO-01	-3.18	5.83	8.99
VLR-01	-26.11	8.09	34.19
VLV-01	-34.54	7.83	42.63
VLW-02	34.87	-10.44	-46.46
VRS-05	11.52	17.7	6
VRS-101	-1.18	7.78	8.75
VRS-201	8.25	18.73	10.24
VRS-202	11.52	17.7	6
VRV-01	-18.37	1.94	20.09
VTM-01	13.41	5.53	-8.16
VTM-01-S	13.41	5.53	-8.16
WAP-01	-12.32	23.22	35.54
WAV-01	-21.25	4.1	25.21
WAV-02	-23.25	3.8	27.05
WAV-03	-33.3	-2.73	30.57
WAV-04	-15.33	7.29	22.62
WAV-06	-16.27	17.24	33.52
WAV-09	-6.76	10.63	17.39
WAV-10	-6.38	10.41	16.76
WAV-11	-6.66	12.72	19.35
WAV-12	-2.8	13.07	15.87
WAV-13	-4.92	6.42	11.38
WAV-14	-2.9	15.26	18.1
WAV-14-S	-2.9	15.26	18.1
WAV-14-S	-2.9	15.26	18.1
WAV-17	-42.18	18.06	60.24
WAV-17-S	-42.18	18.06	60.24
WAW-01	-6.69	3.29	10.18
WDL-01	-25.07	-6.87	18.2
WDV-04	19.94	22.54	2.31
WDV-05	33.72	21.94	-12.12
WED-01	36.74	5.57	-31.17
WED-02	36.14	4.32	-31.82
WEP-01	-10.2	-7.76	2.43
WGF-01	-33.37	-16.68	16.63
WHM-01	-10.8	-45.03	-34.23
WIR-01	-14.3	0.27	14.57
WIT-03	9.59	9.23	-0.36
WRF-01	2.94	-0.64	-3.58
WRG-01	-4.38	14.38	18.76
WRM-01	15.02	8.66	-6.51
WRM-02	-18.81	-14.71	4.1
WRM-03	-4.42	7.61	11.96
WRW-01	0.31	20.34	20.01
WSE-01	-56.67	-22.16	34.42
WSF-01	-40.84	-29.11	11.73
WSM-01	-2.49	16.44	17.98
WTD-01	-12.92	11.49	24.42
WTD-01-S	-12.92	11.49	24.42
WTD-01-S	-12.92	11.49	24.42
WTD-02	-14.87	20.72	35.61
WWK-01	0.98	27.37	26.39
WWN-01-S	-2.71	10.32	13.03
WWN-02	-3.88	11.8	15.68
WWN-03	-35.79	-22.33	13.46
WWS-01	-10.57	28.86	39.43
WYH-01	-30.58	6.57	37.14
WYK-04	1.81	14.93	13.12
WYK-04-S	1.81	14.93	13.12
WYK-06	-17.71	13.01	30.74
WYK-09	-15.97	10.2	26.2
WYK-10	-10.39	13.4	23.82
WYK-11	-14.28	12.22	26.55
WYK-13	-6.1	5.86	11.96
WYK-14	-7.51	3.88	11.39
WYK-15-S	-8.35	6.35	14.61
WYK-15-S	-8.35	6.35	14.61
WYK-16	-3.7	7.23	10.91
WYK-17	-9.96	4.04	14
WYK-17-S	-9.96	4.04	14
WYK-17-S	-9.96	4.04	14
WYK-21	-12.13	-22.04	-9.89
WYK-22	-14.53	9.8	24.23
WYK-24	-12.66	1.33	13.85
WYK-26	-12.44	-0.43	12.01
WYK-27	-14.93	0.58	15.42
WYK-29	-4.67	12.28	16.94
WYK-31	-12.71	1.79	14.64
WYK-33	2.22	16.44	14.21
WYK-33-S	2.22	16.44	14.21
ZDW-01	-21.07	35.5	56.57
ZDW-02	-23.09	20.44	43.52
ZDW-03	-20.67	26.68	47.36
ZEW-01	15.72	-8.71	-24.36
ZLN-01	7.78	-1.92	-9.7
ZLV-01	-1.86	11.86	13.35
ZLV-02	-0.96	13.1	13.52
ZLV-03	0.45	13.12	12.45
ZLV-05	-3.17	13.83	16.75
ZND-01	34.66	25.71	-8.92
ZND-04	36.64	14.19	-22.41
ZND-06	37.66	13.67	-23.91
ZND-06-S1	37.66	13.67	-23.91
ZND-07	29.6	26.67	-2.91
ZPD-01	20.69	6.96	-13.87
ZPD-12	20.64	10.91	-10.09
ZPD-12-S1	20.64	10.91	-10.09
ZRP-01	2.76	24.97	22.2
ZUR-01	51.47	-13.25	-64.72
ZUW-02	5.8	12.55	6.33
ZVH-01	23.98	-24.49	-48.45
ZVH-01-S1	23.98	-24.49	-48.45
ZVN-01	-6.86	-20.97	-14.1
ZVN-13	-33.21	-114.36	-81.13
ZWA-01	-41.23	-47.72	-6.49
ZWO-01	-13.68	25.49	39.14
Average	**-3.33**	**6.53**	**9.90**
StDev	**19.82**	**30.54**	**32.04**

Table 9-1 Well Residuals of top, base and thickness of the Brussels Sandstone

Appendix 2 Well Panel Sonics South NL

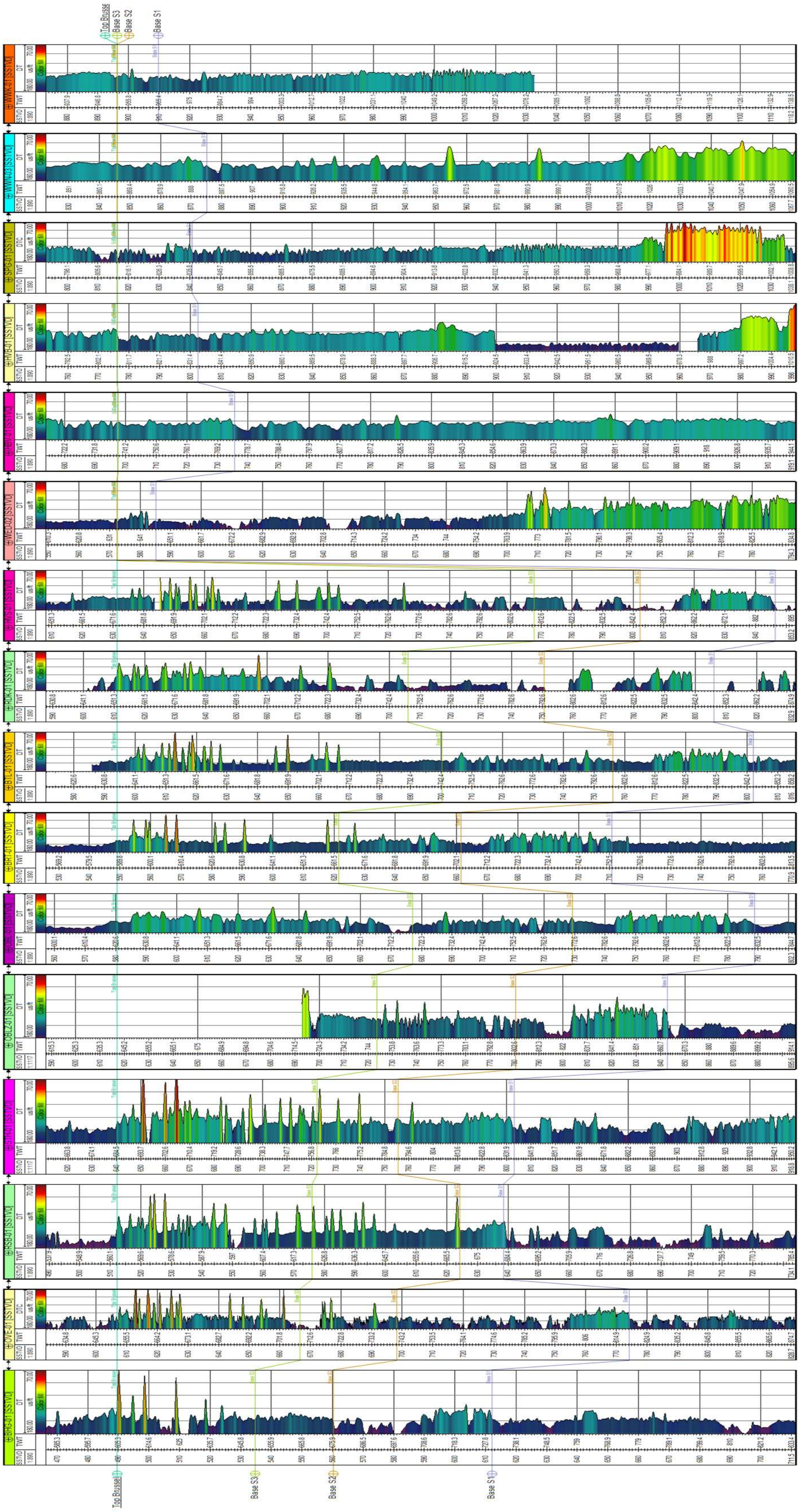

Figure 9-1 W-E well section showing sonic logs. Evident are the high velocity spikes in the S3 sequence. Top Brussels Sandstone is in the west mostly close to an increase in velocity. In the East where sequence S1 is only present a decrease in velocity is most common close to top Brussel Sand.

Appendix 3 Maps

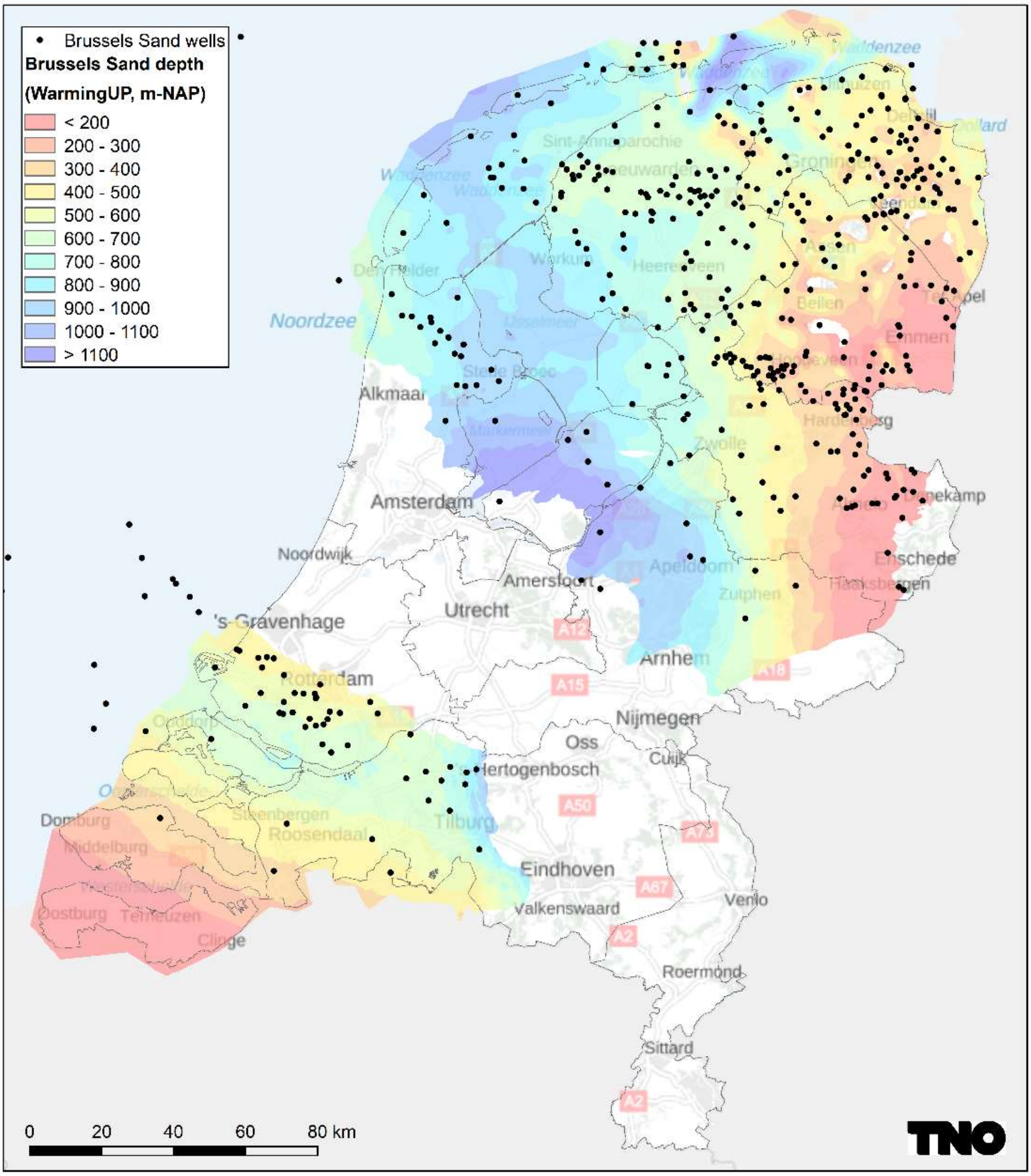

Figure 9-2 Depth of the top of the BSM

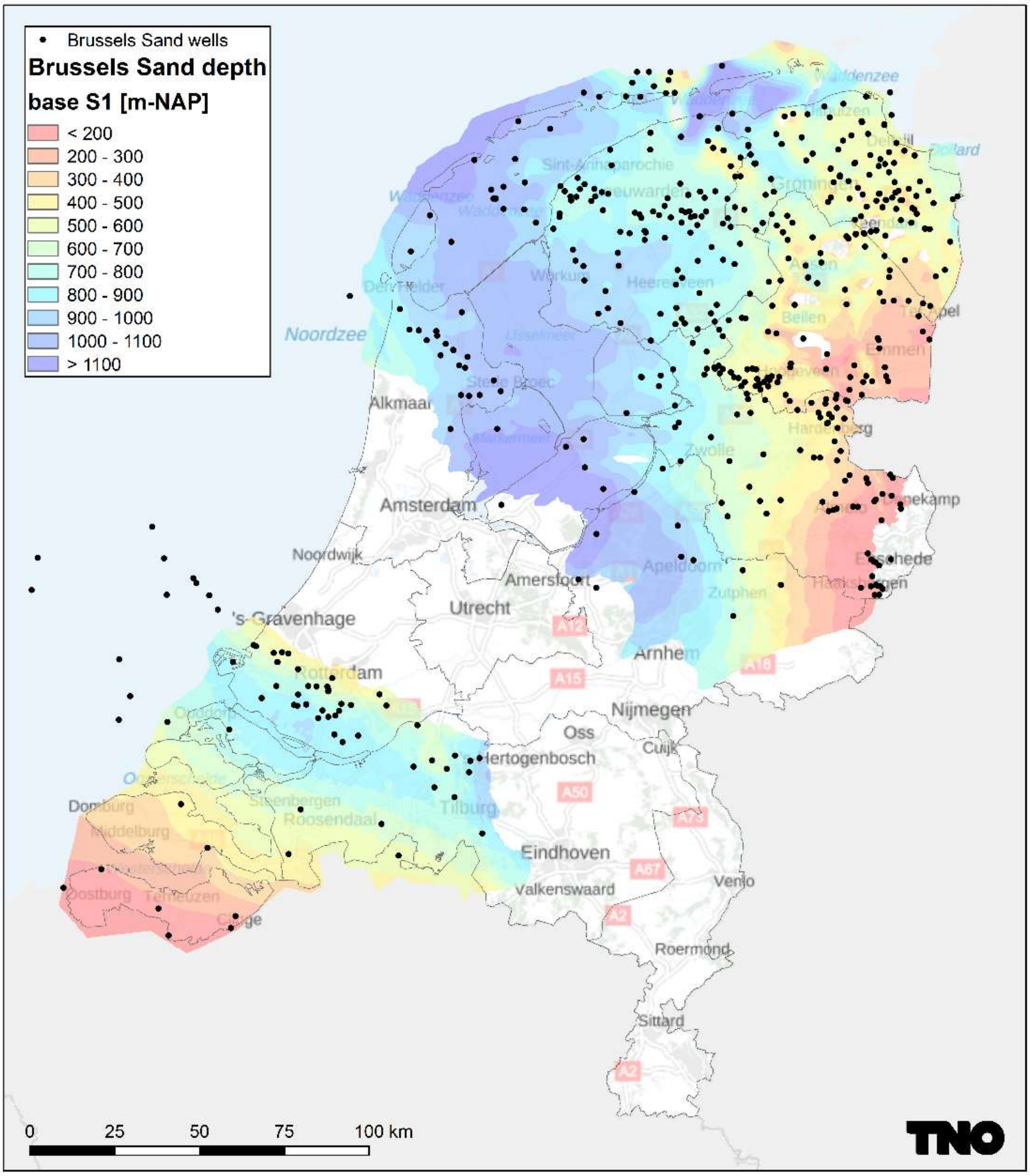

Figure 9-3 Depth of the base of the BSM(base of cycle S1)

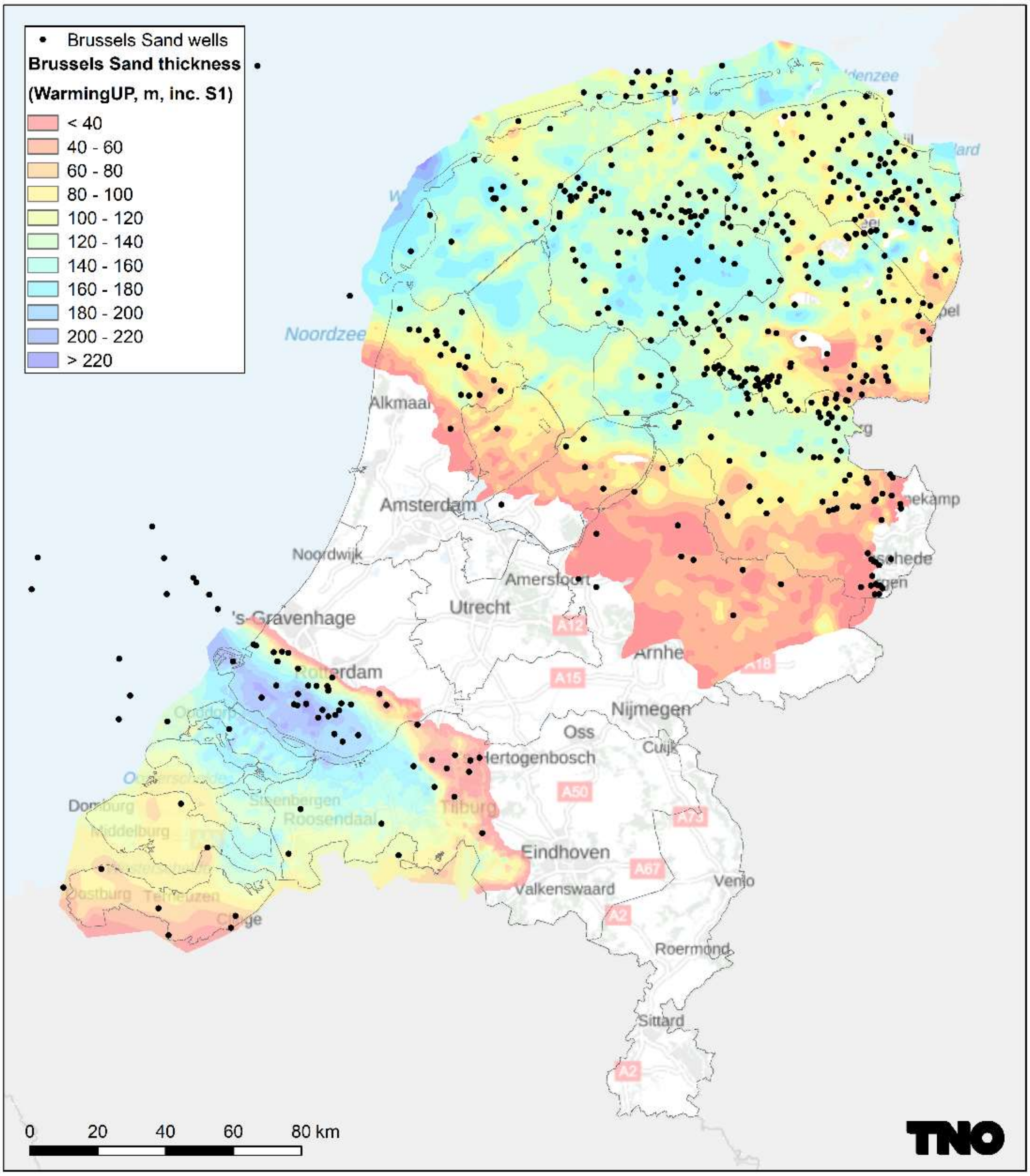

Figure 9-4 Thickness of the BSM including the S1 cycle

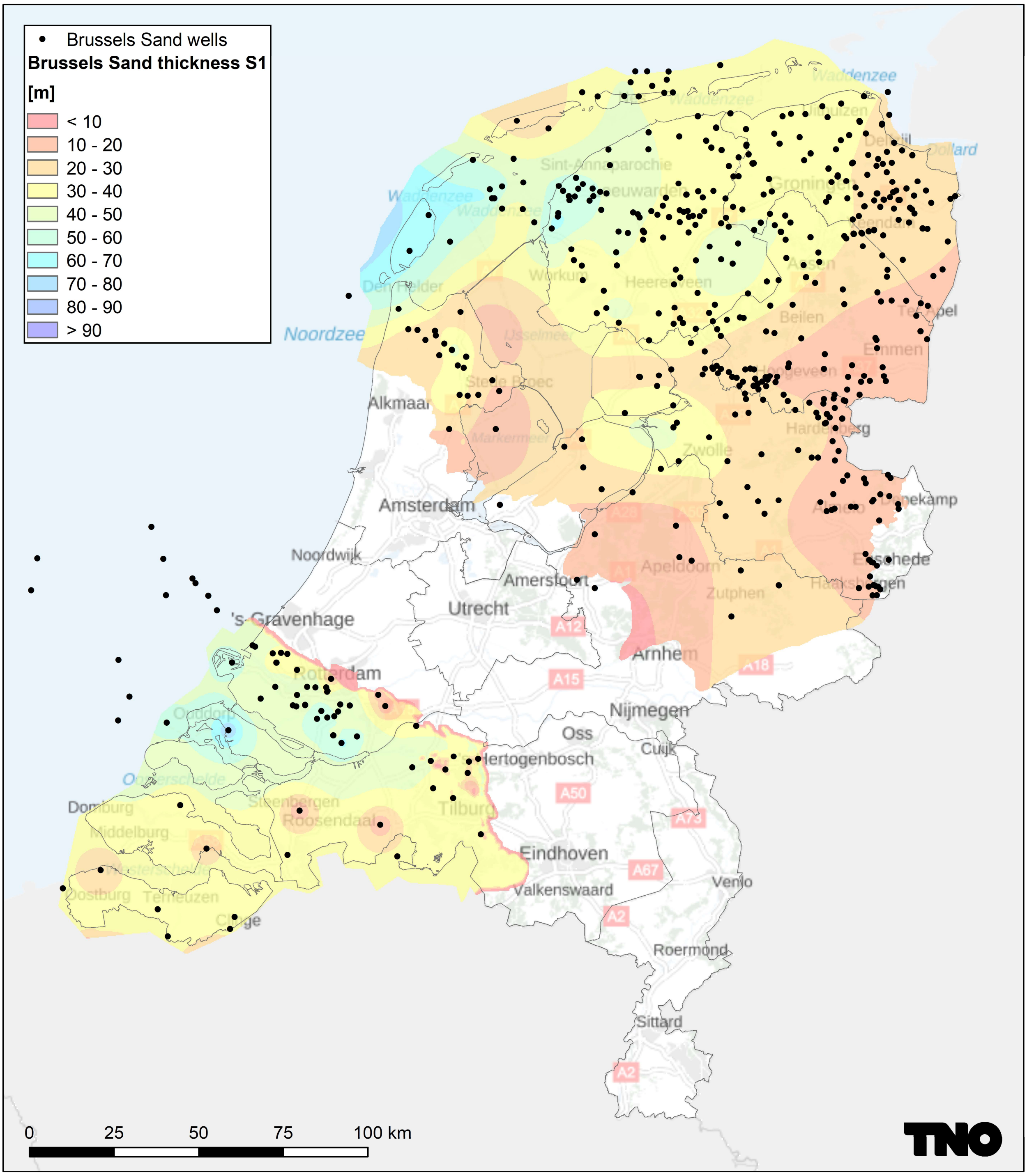

Figure 8 5 Thickness of the S1 cycle

Appendix 4 Seismic Composite Sections

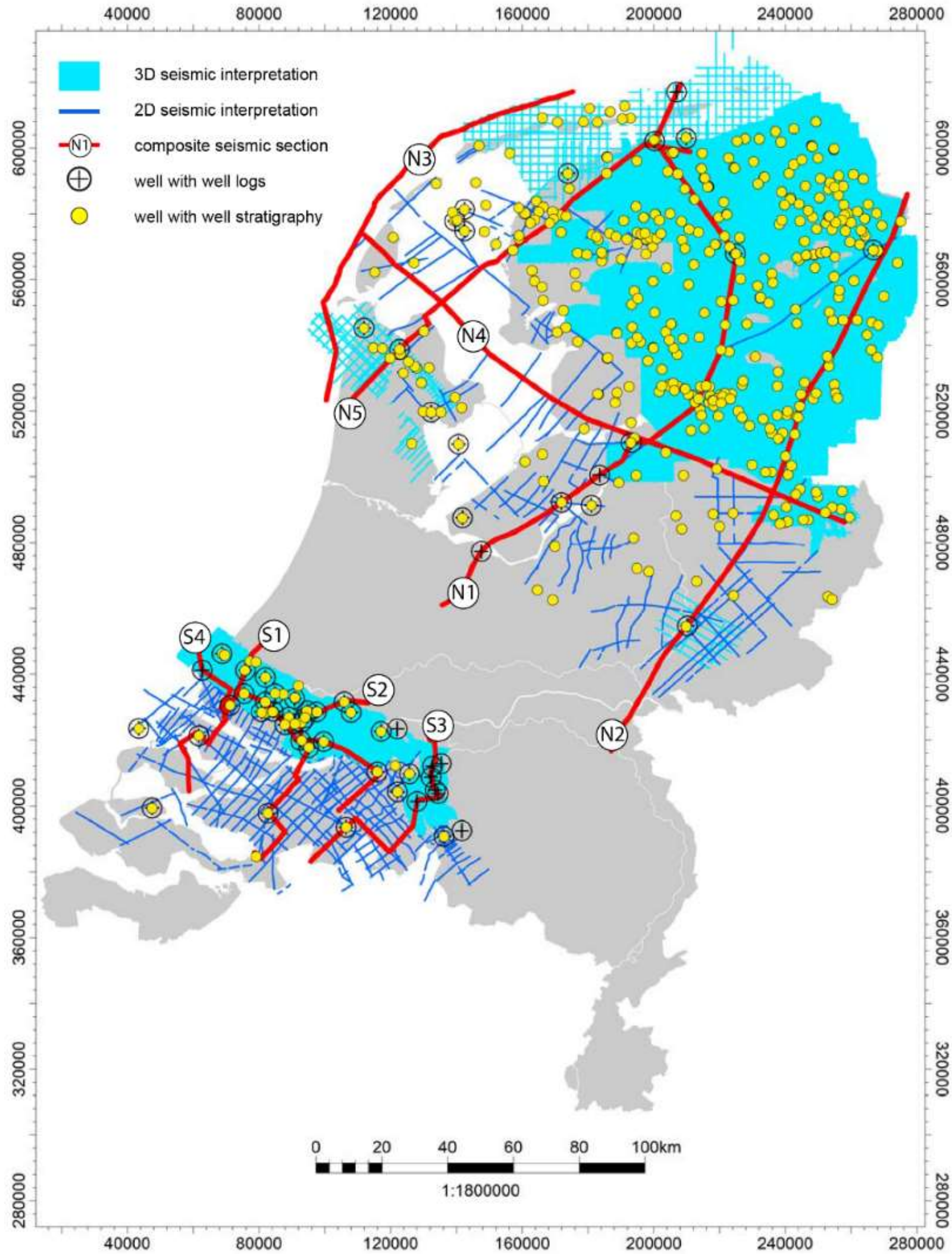

Figure 8 6 Map displaying locations of seismic composite sections (S1-4 and N1-5).

WARMINGUP
Innovatief Duurzaam Warmtecollectief

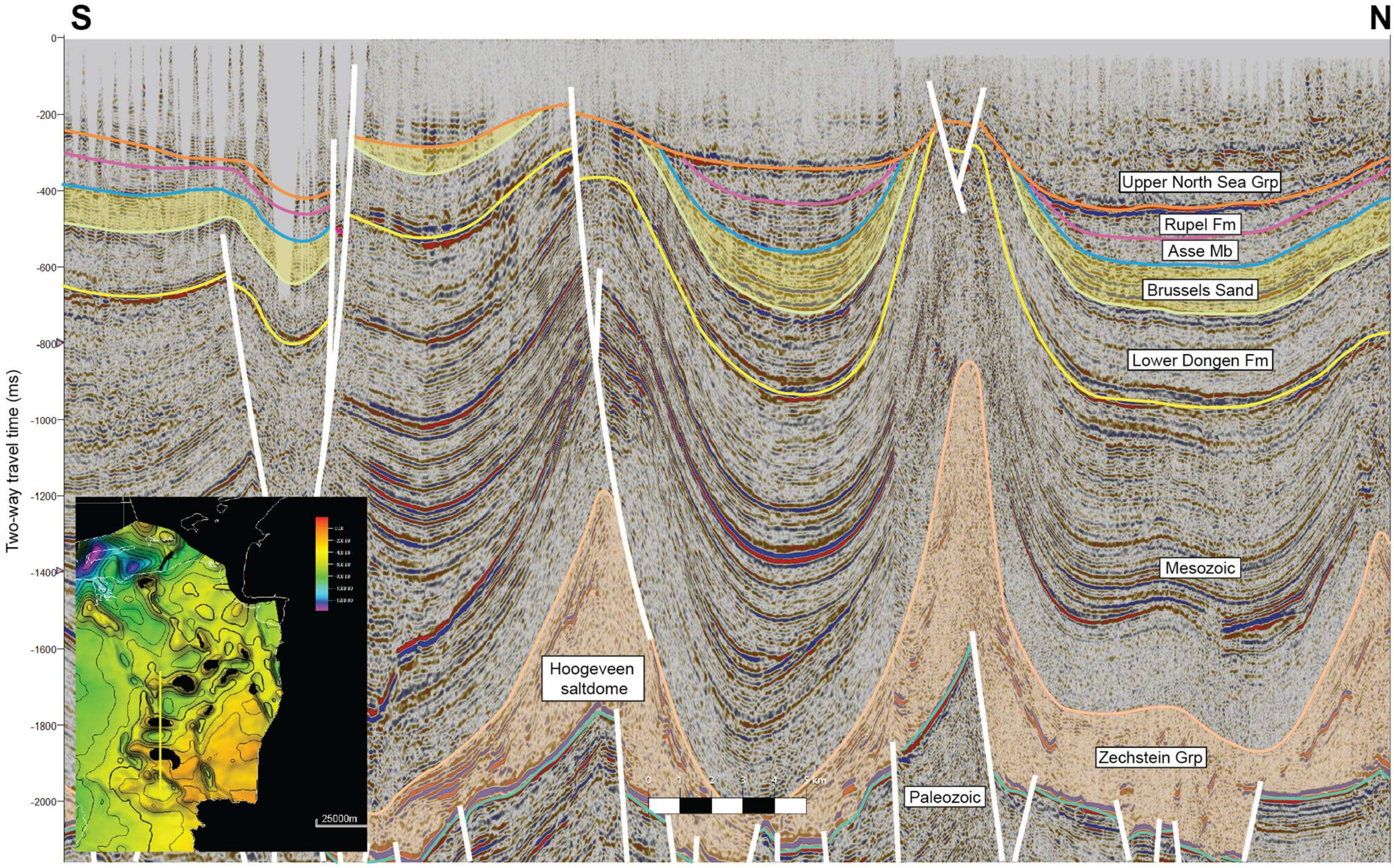

Adres
Princetonlaan 6
3584 CB Utrecht

Postadres
Postbus 80015
3508 TA Utrecht

Telefoon
088 866 42 56

E-mail
contact@warmingup.info

Website
www.warmingup.info

21 december 2020